CHEMICAL CHARACTERIZATION OF CALDANAEROBACTER SUBTERRANEUS SUBSP. TENGCONGENSIS HEME–NITRIC OXIDE /OXYGEN BINDING PROTEIN

A Thesis Submitted to the Graduate School of Engineering and Sciences of İzmir Institute of Technology in Partial Fulfillment of the Requirements for the Degree of

MASTER OF SCIENCE

in Biotechnology

by

Merve ERDAL

December 2020

İZMİR

ACKNOWLEDGMENTS

First and foremost, I would like to express my sincerest gratitude to my supervisor Assoc. Prof. Dr. Nur Başak SÜRMELİ ERALTUĞ for her help, care and support throughout my thesis. I would like to thank Assoc. Prof. Dr. Nalan ÖZDEMİR for scientific advice and support.

I am thankful to my lab mates; Ekin KESTEVUR DOĞRU, Gülce GÜRALP, Fatmanur BOSTAN, Alper ŞAHİN, Muhammet Semih BAŞLAR , Dilara TİLKİOĞLU and Tuğçe SAKALLI for their precious friendship and generous help. I also appreciate to the Özdemir Laboratory members for their contributions and support. Especially I would like to express great thanks to my cousin Hazal AKSOY for her great help and advice.

Finally, my deepest appreciations and love goes to my father, mother and sister; Vedat ERDAL, Gülten ERDAL and Berna ERDAL TOPLU. I thank my family from the bottom of my heart as they have supported me at every single decision I have taken in my life. I am very grateful to they never gave up to support, defend and uplift me. It would not be possible to come this far without their unconditional love and ingeniously guidance.

ABSTRACT

CALDANAEROBACTER SUBTERRANEUS SUBSP. TENGCONGENSIS HEME–NITRIC OXIDE /OXYGEN BINDING PROTEIN

Hemoproteins, which contain the heme prosthetic group , take part in different biological processes in many stages of life. Their ability to catalyze important biosynthesis reactions makes them good candidates for understanding and elucidating complex mechanisms for biocatalysis. In this study, the catalytic properties of thermophilic *Thermoanaerobacter tencogensis* nitric oxide/oxygen binding protein, a heme protein reshaped by rational design, were investigated and chemical characterization was carried out.

The peroxidase activity of the enzyme was investigated by the oxidation reactions of guaiacol, amplex red and 2,2'-azino-bis(3-ethylbenzthiazoline-6-sulfonic acid (ABTS). Kinetic parameters of the reactions were determined. These obtained results demonstrated that, in the presence of H_2O_2, wild type and Y140H T*t*H-NOX proteins are able to catalyze oxidation reactions of guaiacol, Amplex red and ABTS. Comparison of the kinetic parameters showed that Y140H mutant catalyzed the guaiacol and ABTS oxidation 3-fold and 15 -fold faster than wild type enzyme, respectively.

The stability of T*t*H-NOX proteins were investigated in the presence of organic solvents. Results were demonstrated that WT T*t*H-NOX was more stable than Y140H mutant in the presence of organic solvents

In addition to these, for the first time, thermophilic T*t*H-NOX proteins were immobilized with a novel enzyme immobilization method and organic-inorganic hybrid nanostrucrures were obtained. Copper ion incorporated T*t*H-NOX-based hybrid nanoflowers were synthesized at different pH values. SEM and EDX analysis of T*t*H-NOX-based hybrid nanoflowers proved that free T*t*H-NOXs were immobilized successfully.

ÖZET

CALDANAEROBACTER SUBTERRANEUS SUBSP. TENGCONGENSIS HEM – NİTRİK OKSİT / OKSİJEN BAĞLAYICI PROTEİNİNİN KİMYASAL KARAKTERİZASYONU

Hem prostetik grubuna sahip olan hemoproteinler, yaşamın pek çok aşamasında farklı biyolojik süreçlerde yer alırlar. Önemli biyosentez reaksiyonlarını katalize etme yetenekleri, onları biyokataliz için karmaşık mekanizmaları anlamak ve aydınlatmak için iyi adaylar yapar. Bu çalışmada rasyonel tasarımla yeniden şekillendirilen bir hem proteini olan termofilik *Thermoanaerobacter tencogensis* nitrik oksit/oksijen bağlayıcı proteininin katalitik özellikleri incelendi ve kimyasal karakterizasyonu yapıldı.

Enzimin peroksidaz aktivitesi, gayakol, ampleks kırmızısı ve 2,2'-azino-bis(3-etilbenztiazolin-6-sülfonkasit)(ABTS) in oksidasyon reaksiyonları ile araştırıldı. Reaksiyonların kinetik parametreleri belirlendi. Sonuçlar hidrojen peroksit varlığında doğal ve mutant Y140H T*t*H-NOK proteinin gayakol, Ampleks kırmızısı ve ABTS oksidasyonlarını kataliz edebildiğini gösterdi. Kinetik parameterlerin karşılaştırılması Y140H mutantının gayakol oksidasyonunu 3 kat ve ABTS reaksiyonunu da 15 kat olmak, üzere doğal T*t*H-NOK tan daha hızlı gerçekleştirdiğini gösterdi. T*t*H-NOK proteinlerinin organik solventlerdeki stabilitesi araştırıldı ve sonuçlar doğal T*t*H-NOK proteinin organik solventlerin varlığında Y140H mutantından daha stabil olduğunu gösterdi.

Bu çalışmaların yanısıra, ilk kez termofilik T*t*H-NOK proteinleri yeni bir enzim immobilizasyon yöntemi ile immobilize edilerek organik-inorganik hibrit nanoyapılar elde edildi. Bakır iyonları ve T*t*H-NOK proteinleri kullanılarak farklı pH aralıklarında çiçek benzeri şekillere sahip T*t*H-NOK -inorganik hibrit nano (T*t*H-NOK-ihN) yapılar sentezlendi. SEM ve EDX analizleri sonucunda başarılı bir şekilde serbest T*t*H-NOK enzimlerinin immobilize edildiği gözlendi.

TABLE OF CONTENTS

LIST OF FIGURES

Figure **Page**

Figure **Page**

LIST OF TABLES

Table **Pages**

CHAPTER 1

INTRODUCTION

1.1.Biocatalysis and Biocatalyst

Enzymes are protein biopolymers found in all living cells that consist of 20 natural amino acids. Within a cell, enzymes act as biocatalysts driving a lot of chemical reactions and coordinating various cellular functions. Especially, they are crucial for living cells in the way of their survival and reproduction. These significant biocatalysts evolved in nature by themselves to achieve the speed needed in reactions and to maintain the necessary coordination of these chemical reactions. Biocatalysts enhance the development of life. In nowadays technology, biocatalysts are being modified to exceed the limit of nature and served more powerful assists.

Numerous biocatalysts have been utilized in food industry, cleaning chemicals and medical processes for years (Bornscheuer and Kazlauskas,2006). Despite their potential of practical applications such as animal feed, pharmaceuticals, bulk and fine chemicals, detergents, fibers for clothing, hygiene, and environmental technology, natural enzymes are not often convenient for practical uses., Enzyme properties such as, suboptimal temperature, pH, isoelectric point, substrate specificity, reaction mechanism, and molecular stability must be modified, improved or tailored to gain more suitable features (Luetz, Giver and Lalonde, 2008).

Today, biotechnology offers to increase the potential of the enzyme engineering which is aimed to gain selectivity, high stability, substrate specificity and catalytic activity. Recombinant DNA technology has offered a complete solution for cloning and expressing a gene of interest. In order to make the enzymes more suitable for industrial use, many enzymes are being screened in their natural sources, random mutations are being tried and enzyme immobilization are being studied (Dinçer and Telefoncu, 2007;).

The utilization of biocatalysts for chemical processes was possible through the

development of design tools such as; rational design and directed evolution. Though these processes, tailor-made biocatalysts are being created from wild type enzymes (Bornscheuer and Kazlauskas, 2006). Immobilized enzymes offers a heterogeneous catalytic system for continuous and repeated operation that is more robust and cost effective.

By work through studies that provide understanding and enlightenment of the structure and functions of enzymes, it has been possible to design enzymes with new functions, and as a result, biocatalysis has developed .

1.1.2 Advantages and Disadvantages of Biocatalysis

Biocatalysis is the use of biomolecules such as enzymes or whole cells catalysts in chemical reactions. Enzymes offer several attractive features as in catalysts for organic synthesis. The most significant advantages of a biocatalyst are its high chemoselectivity, regioselectivity and enantioselectivity. Chemoselectivity refers to the enzymes that often catalyze only one of functional group reactions and others can remain in the molecule untouched when similarly-reactive functional groups are present in a molecule. “Regioselectivity” is another useful property displayed by many enzymes. They can differentiate functional groups that are in different regions. So, other identical or nearly identical moieties do not effected and can still remain in the molecule. (Animesh Goswami and Stewart, 2016)

Except glycine all amino acid contain at least one chrial center and for this reason, enzymes are intrinsically asymmetric catalysts. Their asymmetrical nature allows biocatalysts to be enantioselective and preferably, they are able to transform only one stereoisomer of a compound consisting of diastereomers or mixture of enantiomers (Karlheinz Drauz, 2012).

Biocatalysis have been used for the one- step production of aspartic acid , in multi-step production of alcohol and cheese (Johannes et al.,2006),the oxidation of ethanol to acetic acid (Wandrey et al., 2000) , the production of acrylamide (Asano et al., 1982) and more of the same. Thanks to advances in the understanding of protein structure and function, the range of biocatalytic applications have been increased over the years through .

The unique characteristics of biocatalysyts are highly desirable and advantageous for industrial and commercial applications. These features provide higher yeilds, fewer side reactions, easier recovery, good separation and production of pure compounds.

Biocatalysts are enzymes and enzymes are proteins that are biodegradable; so, biocatalytic processes are "greener" and sustainable. The use of biocatalysts obtained from immobilized enzymes does not cause environmental hazards (Mohamad et al., 2015). Since the use of solvents in biocatalytic processes is reduced and aqueous solutions are used, waste disposal problems cannot occur. They stand in need of mild operating conditions and low energy input. Thanks to their low energy cost, they provide lower greenhouse gas emissions to the environment (Rozzell, 1999).

Despite all these advantageous properties, biocatalysts are not seen as the first alternative in the industry due to some preconceived ideas and misconceptions:

- "Enzymes are very expensive"

The important point in the margin is that not cost of the enzymes itself; it is the cost-contribution of the enzyme to the final product. For example, the cost contribution of a transaminase for the production of fluoro-L-phenylalanine, which may have a selling price of $500 per kilogram or more, is only about $20±30 per kilogram. This cost contribution is far less than that of the raw materials (Rozzell, 1999).

- "Enzymes are too unstable"

It is known that a lot of enzymes are unstable at high temperatures or in extreme pH conditions. On the other hand, many enzymes display excellent stability when they immobilized. In adittion to that, the development of thermostable enzymes by isolation from thermophiles or by directed evolution give hope to create even more robust catalysts for industrial application. (Trudeau et al.,2014; Diaz et al.,2011).

- "Productivity is too low. "

This misconception came from the fact that, the fermentation process have low

volumetric productivities because of it is involves a path of carbon precursors (Rozzel,1999). Thanks to immobilization of enzymes, their productivities have been incrased (Homaei et al., 2013; Mohamad et al., 2015).

- " Redox cofactors cannot be recycled effciently. "

Contrary to popular belief, redox cofactors such as nicotinamide have been recycled efficiently by using three different method. First one is the use of a coupled reaction that the catalysis of synthesis of a product from one substrate and the cofactor regeneration reaction as second substrate is done by an enzyme, which utilizes the reduced and oxidized forms of that cofactor (Lemière et al., 1985). Phenyllactic acid is the product of the reduction of phenyllactate dehydrogenase by using nicotinamide adenine dinucleotide (NADH). NADH is generated by using ethanol and alcohol dehydrogenase (Rozzell, 1999). In the second method, macro-molecularized cofactor in a membrane reactor, such as hollow-fiber, flat membrane and packed- bed reactors, have been used (Liu and Wang,2007) . The NAD^+ cofactor has been recycled by using this method. The third one, whole cell with dehydroganes enzymes and a cofactor is used. Then coafactor is recycled by the additon of a carbon source which provides reducing equvalents for the degeneration of the cofactor and maintenance energy to the cell (Servi,1990).

- " Enzyme can only produce one or two possible enantiomers. "

According the studies biocatalysts were able to convert a racemic mixture to a new product with different chemical and physical properties. These new product can be separated with respect to appropriate seperation method (Liese et al., 2006).

1.2. Hemeproteins

Heme is the most salient and versatile class of cofactors utilized in biology. It is one of the most important tetrapyrole cofactor and a widely used metalloprophyrin in nature. In the nature, heme proteins are found from the archaea to higher organisms and they have operational importance used to carry out myriad of diverse biological functions. All hemoproteins carry iron (Fe) portoporphyrin IX as a prosthetic group and

also catalyzed both reductive and oxidactive chemistry (Poulos, 2014). Fundamentally, heme structure consist an Fe ion bonded to four central nitrogen atoms of a porphyrin ring. Mostly observed hemes are heme b and heme c. Among of these two, the heme b is most abundant. Heme c has covalent bond between the vinyl groups and cycteine residues of proteins; on the other hand, heme b forms a non covalent bond with protein (Bowman and Bren, 2008).Heme b, also called protoheme, has methyl groups at positions 1, 3, 5, and 8; vinyl groups at positions 2 and 4 and propionates at positions 6 and 7 on the macrocycle (Reedy and Gibney, 2004).

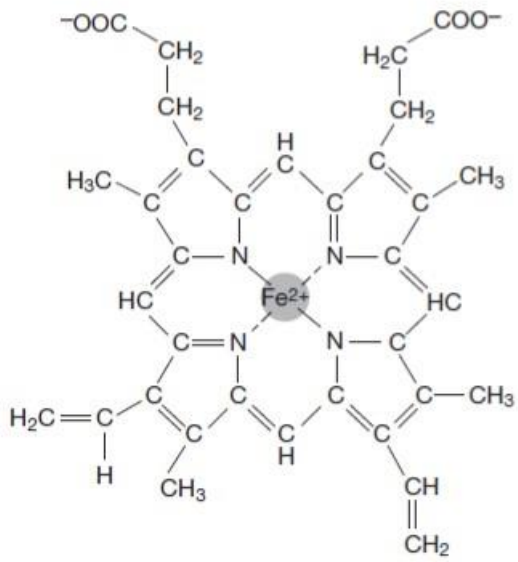

Figure 1.1. Chemical structure of iron-protoporphyrin IX (hemin) (Everse, 2013).

Hemeproteins not only have significant importance for the cellular processes of most of the organisms but also essential for many life forms accross domains of life. Heme proteins are inseparable part of a great many crucial biological processes including steroid biosynthesis (Granick and Kappas,1967), aerobic respiration(cytochromes), and even programmed cell death(Ow et al., 2008). Some heme binding sites was evolved by the nature within a diversity of protein scaffolds to achieve such many kinds of tasks as electron transfer (Shichi, 1969) substrate oxidation(P450enzymes)(Guengerich, 2007) ,and oxygen transport(globins) (Reichlin,1972). Some heme proteins have the importance of sensing the diatomic small molecules like carbon monoxide (CO), nitric oxide (NO) and oxygen (O_2) (Jain and Chan, 2003).

According the heme-binding domains, four heme-based sensors were

identified. Their classification were made based on ligand specificity and performance of sense, either CO, NO or O_2.Two domains that are specialized to detect O_2 are found in prokaryotes. One of them, myoglobin - like heme domain that is contained an aerotaxis-regulating protein from HemAT (Aono et al., 2002). Second one is the heme-PAS domain found in the histidine kinase containing protein from FixL. (Gilles-Gonzalez et al., 1991).

Third heme - domain, specialized for CO sensing, is CooA protein found in Rhodospirillum rubrum that have function in regulation of the genes involved in CO oxidation (Shelver et al., 1997). Last heme- domain is found in soluble guanylate cyclases (sGCs) and can sense the nitric oxide (NO) (Jain and Chan, 2003).

In nature great number of heme proteins act as enzyme. The most common ones are peroxidases and catalases . Most peroxidases can oxidize a variety of substrates of extensively different structures with hydrogen peroxide or an organic peroxide (Everse, 2013).

In the action mechanism of the heme peroxidases, at first step enzyme is oxidized by the peroxide and is yielded the compound I which is a ferryl porphyrin cation radical. ($Fe^{IV} = Opor.^{\bullet+}$) Then, this intermediate compound I reduced to the ferric compound II , ferryl porphyrin ($Fe^{IV} = Opor$). Removal of a second electron from compound II leads to restore the native ferric enzyme (Everse, 2013).

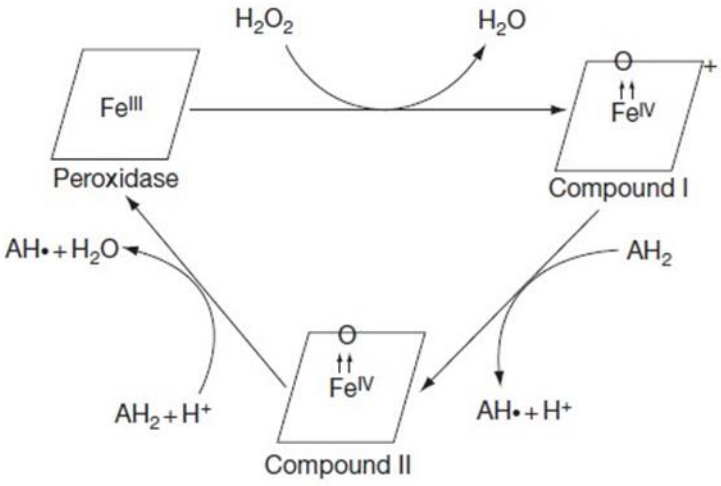

Figure 1. 2. Action mechanism of Peroxidases (Everse, 2013).

Catalases are able to neutralize the hydrogen peroxide which is formed in vivo

by diverse oxidases and other enzymes. Basically, the enzyme catalyzes the dismutation of 2 mol of hydrogen peroxide into 1 mol of oxygen and 1 mol of water. Reaction mechanism is partially similar with peroxidases. Binding of a mole of H_2O_2, leads to the production of a compund- I type intermediate and one mole of water is released afterwards. After the reaction with one mole of H_2O_2 second time, one mole of oxygen is produced and the native enzyme is regenerated (Everse, 2013). Function of heme is importantly affected by the amino acid residues that covered the iron protoporphyrin IX. Especially, residues around the axial ligands of heme lead to diversify.

Studies have shown that, all peroxidases have a histidine ligand (Gajhede, 2001) and all catalases have a tyrosine ligand Mate et al, 2001) . NO synthases (Rosenfeld,2001), Cytochromes P450s (Li H.,2001) and Chloroperoxidases (Sundaramoorthy,2001) have cysteine axial ligands. Not only axial ligands but also distal ligands varies among hemeproteins. The proximal histidine ligands of peroxidases make hydrogen bonding with an aspartate residue(Gajhede,2001). This bond provides an increase in the electron density on the Fe ion (Poulos,1996). Proximal tyrosine ligands of catalases make hydrogen bonding with arginine (Mate et al.,2001).Functional and activity affects of axial and proximal ligands of hemeproteins have been invastigated. Axial and proximal ligands have "push-pull" effect. In the push effect, ligand stabilizes the oxidation state of compound I and II by hydrogen bonding with increasing aspartate residue . Pull effect occurs when the distal side has histidine and arginine residues which enhance the heterolytic reactivity (Rydberg et al.,2004).

1.2.1. Heme-Nitric Oxide/Oxygen (H-NOX) binding domain

Nitric oxide (NO)is a free radical and is an important signaling molecule in eukaryotes. In mammals, NO play an important role in a lot of physiological processes including blood vessel relaxation, myocardial function, cerebral blood flow, synaptic plasticity in the brain, platelet aggregation and egg fertilization (Hare and Colucci, 1995) (Toda and Okamura, 2003) (Denninger and Marletta, 1999). NO has a sensetive receptor called as soluble guanylate cyclase (sGC). sGC is a heterodimeric heme sensor and can selectively binds NO by its ferrous ion. Production of cyclic guanosine monophosphate (cGMP) from guanosine triphosphate (GTP) starts when NO binds with the sGC. cGMP

is the secondary messenger which is in turn mediates the down signalling events such as Ca2+ channels, kinases, and phosphodiesterases; resulting in NO-specific regulation of biological processes (Underbakke and Surmeli, 2013). Also binding of NO results in the dissociation of the proximal histidine; a 5-coordinate (5C) active complex be formed. sGCs very sensetive to NO even at high oxygen concentration. For this reason, even a weak oxygen binding can cause the blockage of the whole NO signalling pathway (Boon and Marletta, 2005). In procaryotes, NO regulates bacterial communal behavior, motility and quorum sensing, biofilm formation and symbiosis (Plate and Marletta, 2013) (Carlson and Vance, 2010) (Hossain et al., 2018).

H-NOX proteins firstly recognized in a bioinformatic search for sequence homologs of the heme-binding domain of the mammalian sGC. Iyer et al. identified, for the first time, a new family of hemeproteins in bacteria with substantial homology (15-40 %identity) to the heme domain from rat sGC (Iyer et al., 2003). These identified heme domains are all about 190 amino acids, which have particularly high identity to sGC in and around the heme-binding region. Especially, several amino acids were definitely conserved and can be considered signatures of the family. Beside the universally conserved histidine heme ligand, a YxS/TxR motif is conserved which is important for coordinating the haem propionate side chains.(Schmidt et al.,2004). This motif, along with the proline residue, is now known to be important for maintaining a unique haem structure in this family.

Cloning and spectroscopic characterization clarified that heme domains which obtained from facultative aerobes, forming 5-coordinate NO complexes and rigorously excluded O_2 as a ligand .(Karow 2004.) However, hemeprotein obtained from the obligate anaerobe Thermoanaerobacter tengcongensis was shown to have similarities with the globins and forming stable O_2 comlex and also, a 6 -coordinate NO complex. Therefore, this family was named as Heme-Nitric Oxide / Oxygen (H-NOX) binding domain. As seen in Figure 1.3, Yellow ones are conserved residues across all H-NOX proteins. Red ones tyrosine residues that required for O_2-binding in the H-NOX family from T*t* H-NOX and it is conserved among the strict anaerobes. Blue ones are Tryptophan 9 and asparagines 74 and their homologous residues in the other strict anaerobes. Phenylalanine 78 is highlighted in green

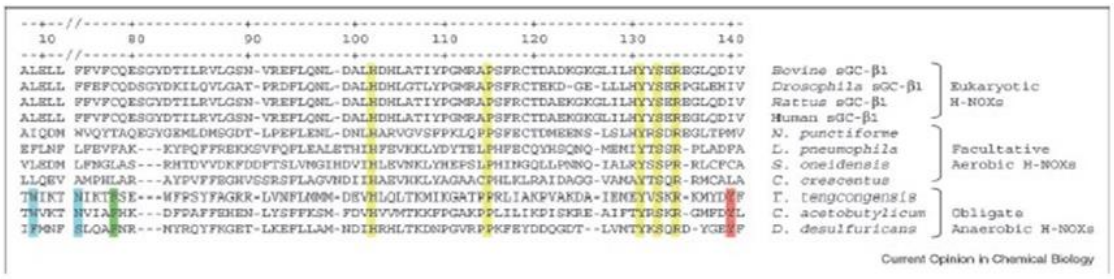

Figure 1.3. Sequence alignment of selected eukaryotic and prokaryotic H-NOX proteins (Boon and Marletta, 2005).

1.2.2. *Thermoanaerobacter tengcongensis* H-NOX (T*t*H-NOX) sensing proteins

Thermoanaerobacter tengcongensis are Gram-negative, obligately anaerobic and extremely thermophilic bacteria which was isolated from a Chinese hot spring. (Xue et al.,2001). It has been suggested that, H-NOX proteins in strict anaerobs have evolved to bind oxygen as a ligand whereas the rest is only selectively bound NO. (Boon and Marletta,2005). The structure of oxygen- binding H-NOX domain from Thermoanaerobacter tengcongensis was reported by Pellicena et. al. in their article. (Pellicena et al., 2008).

This H-NOX family has evolved a novel protein fold which do not have distinct similarity to previously characterized protein folds.T*t*H-NOX has seven alpha helices and four-stranded antiparalel beta sheet. Most important finding about structure is a hydrogen-binding network around the bound ligand, oxygen. This network involves the phenol of tyrosine -140 (Y140) bound to the O_2 and asparagine-74 (N74) and tyrptophan-9 (W9) bound to the phenolic O_2 of Y140 (Boon and Marletta,2005).

By the help of T*t*H-NOX mutagenesis studies, some unique molecular characteristics of the ligand-binding pocket such as heme distortion , heme pocket conformation (Olea et al, 2008), protein dynamics and a ligand entry and exit tunnel network which influences ligand specificity (Plate and Marletta , 2013), were explained. Studies showed that, distal tyrosine, Y140, have important role in O_2/NO ligand discrimination. The mutation of Y140 to leucine was made it clear that Y140 residue is

responsible for O_2/NO ligand discrimination and the formation of stable O_2 complexes in sGCs using a kinetic selection (Boon and Marletta, 2005)

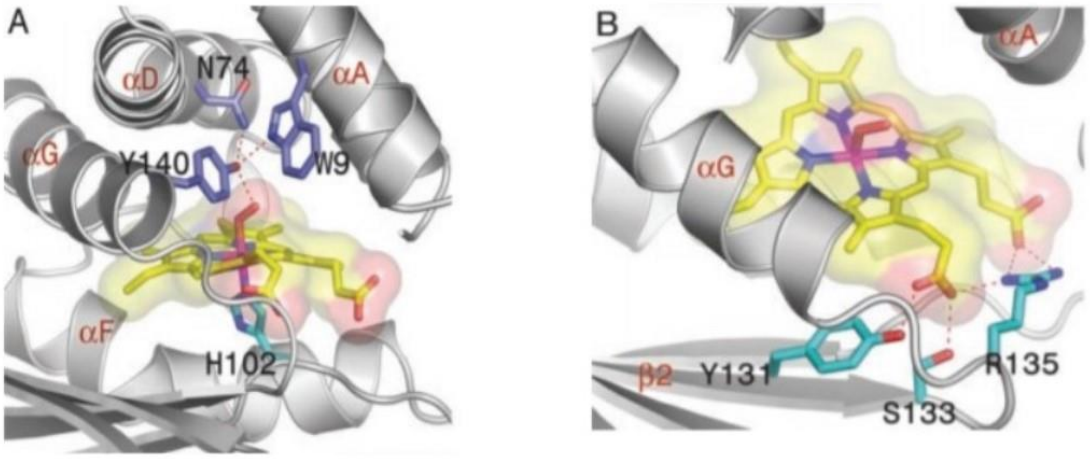

Figure 1.4. Heme environmet of *Thermoanaerobacter tengcongensis* H-NOX (*Tt*H-NOX) Sensing Protein. (A) Tyr-140 is shown hydrogen bonding (red dashes) to the heme-bound oxygen ligand. Trp-9 and Asn-74 interact with Tyr-140. The proximal ligand, His-102, is also shown. (B) The YxSxR motif, corresponding to residues Tyr-131, Ser-133, and Arg-135, coordinates heme propionates (Pellicena and Karow, 2004).

Distal tyrosine creates a hydrogen bound network around the heme with the modulation of O_2-binding affinity in the heme .While absence of the distal tyrosine, the dissociation rate for O_2 much faster than its presence. For this reason, it is responsible for ligand discrimination in H-NOX family. (Boon and Marletta, 2005)

With mutations of Y140 to Alanine and Histidine, the role of the distal tyrosine (Tyr140) in catalysis was investigated (Aggrey-Fynn and Surmeli, 2018). The mutation of Tyr140 to alanine hinders the catalysis of the oxidation reactions. On the other hand, the mutation of Tyr140 to histidine, which is commonly observed in peroxidases,was catalyzed H_2O_2 decomposition and oxidation of 2,2′-azino-bis(3-ethylbenzothiazoline-6-sulphonic acid) by H_2O_2 . Kinetic studies have shown that the Y140H mutation provided the enzyme high catalytic activity. (Aggrey-Fynn and Surmeli, 2018).

1.3. Polyhistidine Tag Protein Purification Systems

Polyhistidine Tags (His-tags), which characteristically involve six or more consecutive histidine residues, are most of the time used in protein purification. His-tagged proteins are easily separated from the cell lysate through the immobilized metal affinity chromatography (IMAC). In IMAC, divalent cations (generally $Ni^{2+,}$ $Co^{2+,}$ Cu^{2+} or Zn^{2+}) are adhered to a solid matrix; around neutral pH the histidine residues form complexes with the chelated metal ions. Afterwards, the desired protein can be eluted through displacement of histidine by addition of imidazole to the mobile phase or changing the pH of the solution. (Bornhorst and Falke, 2000).

Due to His-tags are relatively small in size (~2.5 kDa), common thought are they do not affect the structure and function of proteins (Graslund et al, 2008). Despite this, recent reports assert that, this assumption may be incorrect (Booth et al., 2018; Panek et al., 2013; Sabaty et al., 2013). Although the application of His- tags for protein purification is very useful in increasing the yield and purity of recombinant proteins, ignoring the effects of this technique on native protein structure and function will led to non-reproducibility and confusion in the literature (Majorek et al., 2014).

Over 90% of recombinant proteins are purified through His-tags. Most of the times, the His-tags do not affect the crystallization of proteins and they can even be acted in the formation of crystal contacts. Conversely, the B-factor, which acts the general displacement of atoms in a crystal structure, shows that the presence of a His-tag increases this value compared to structures determined without His-tag; thereby this makes crystallization more difficult. This results also put forward that addition of a His-tag can alter protein dynamics and possibly impact protein activity or function (Booth et al., 2018).

1.4. Enzyme Immobilization

Usually, bigger part of the free enzymes specifically catalyze reactions in the mild experimental conditions such as; neutral pH, room temperature and atmospheric pressure. They perform intrinsic catalytic function to all of the certain substrate or its

functional groups. Although, enzymes very good options the catalization of biological reactions and industrial applications thanks to their substrate specificity, low toxicity and the absence of production of undesirable products, their molecular structure at high temperatures, at acidic or basic pHs and in the presence of organic solvents are easily degredable. This situation stricly limit their use. (Meryam Sardar, 2015) (Zhang et al., 2015). For the re-using in catalysis they cannot be separated and gained from the reaction medium . To address these issues, immobilization techniques are considered.

In the 1960s, enzyme immobilization technologies gave courage to chemists and material scientists for designing of innovative biomaterials for high stabilization of integrated biocatalysts. The term called "immobilized enzyme" was firstly accepted in Enzyme Engineering Conference in 1971 (Hartmeier, 2012).The meaning of immobilization refers to movement-limiting, because binding of free enzymes to support limits their mobility (Kragl et al., 2002). Until the 1990s, continuous progress in this issue enables maintaining the activity of nanostructured materials; immobilized enzymes levels up to that of the native enzymes.

Generally, immobilized enzymes with conventional immobilization techniques exhibit improved stability against environmental changes and are reusable and economic; however these methods are lead to so many disadvantages such as; the lack of effective reusability, an extreme loss of enzymatic activity due to the blocking of the active site of enzyme, difficulties in immobilization, restricted flexibility and mass transfer limitations between the enzyme and substrate (Altınkaynak and Özdemir, 2016). Nowadays immobilization technology is a pretty important area in the biomedical science and biotechnology.

Various bioorganic molecules such as drugs,proteins, peptides, DNA and plant extracts have been succesfully immobilized to the proper support materials. Enzymes show a strong affinity to metal ions as cofactors and generally perform strong stability when they are immobilized on the metal surface (Datta et al., 2012) (Jia et al., 2013) Recent developments provided that enzymes have been immobilized not only on micro sized materials but also immobilized on several types and shapes of nano sized materials such as; nano spheres, fibers, tubes and pores. These supporting materials should have a large surface area ,insolubility in water , biocompatibility and functional groups (Ansari ,2012) (Zhang et al., 2015).

Recently, a novel and elegant approach for the synthesis of immobilized

enzymes in the form of nanoflowers showing enhanced stability and cataliytic activivty (Ge et al..2012). In this novel, immobilization strategy, proteins (enzymes) and metal ions acted as organic and inorganic components respectively, to form hybrid nanoflowers (hNFs).

This simple and one step immobilization occurs by the coordination reactions between amine groups in the backbone of enzymes and copper phosphate nanocrystals. The nanoflower-like structure formation is completed in three consecutive steps; nucleation and formation stage of primary crystals, stage of crystals, formation stage of nanoflowers (Altınkaynak and Özdemir, 2016) . It is proven in the studies that, the hNFs is highly enhanced about catalytic activities and stability in a wide range of experimental conditions (pHs, temperatures and salt concentration, etc.) compared to free and conventionally immobilized enzymes (Altınkaynak and Özdemir, 2016).

This new class of flower-like nanostructures named as 'organic-inorganic hybrid nanoflowers' was exhibited much higher catalytic activity, stability and durability in the biocatalytic reactions compared with free and conventional immobilized forms of enzymes (Ge et al..2012) (Escobar et al., 2017).

1.4.1. Organic-Inorganic Hybrid Nanoflowers

A short time ago , Zare and his coworkers fortuitously found that organic-inorganic hybrid nanoflowers were formed using copper (II) ions as the inorganic component and various proteins as the organic component. (Ge et al., 2012) Hybrid nanoflowers can synthesized simply and they controlled hierarchically- structured flower-like morphology at the nanometer scale; this is very helpful for augmenting the stability, activity, durability, and selectivity of immobilized enzymes compared with those of existing strategies(Ge et al., 2012).

Novel organic- inorganic hybrid nanoflowers have been synthesized in mild reaction conditions at room temperature in aqueous phosphate buffer using recommended synthetic mechanisms, consisting of the initial formation of complexes between nitrogen atoms in amide or amine groups in biomolecules and inorganic metal ions, including copper by the way of the coordination interaction, that drives the nucleation of primary metal phosphate crystals (Tran and Kim, 2018).

With the anisotropic growth highly-branched flower- like structures have been occured, thus in the past couple of years, some enzymes and DNA, including laccase (Somturk and Özdemir, 2015),lipase (Wu and Li, 2014) ,horseradish peroxides (HRP) (Ocsoy, 2015), glucose oxidase (GOx) (Sun et al., 2014) , a-amylase ,urease,trypsin , chymotrypsin , papain and DNA have been prepared in the form of biomolecule-inorganic crystal hybrid nanoflowers which exhibited higher activity than their free counterparts and excellent stability (Cui and Jia, 2017) . Throughout years, hybrid nanoflowers by using copper (II) ions and proteins have been the most studied issue ; by this means, characteristics of them are known very well.

Some kinds of biomolecules such as; peptides, amino acids, DNAs and some kinds of inorganic ions such as; calcium, zinc, cobalt, manganese are the issues that have been also investigated due to the handling of hybrid nanoflowers (Cui and Jia, 2017). Consequently, hybrid nanoflowers are being categorized with respect to the organic or inorganic compound that is used in.

Furthermore, different hybrid nanoflowers enhanced in catalytic performances are developed in order for biotechnology applications which are ranging from biosensing to different types of catalytic applications; even for pollutant removal, protein digestion, biofuel cell and industrial biocatalysis.

This novel approach inspires many researchers and scientists to investigate about the synthesis of protein-inorganic hybrid nanoflowers by using $Cu_3(PO_4)_2$, metal ions such as; $Ca^{2+,}$ $Ca^{2+,}$ Co^{2+}, Ni^{+2}, Zn^{2+}, Mn^{+2} etc. (Bilal and Asgher, 2019) and different types of enzymes. Hybrid nanocomposites with their extensive benefits gained with the help of multiple functionalities of the enzyme/protein and inorganic fraction can be taken part in many industrial uses such as; biocatalysis, environmental management, biofuel production,biofuel cells, biosensors, and bio-related analytical devices (Bilal and Asgher, 2019) .

In industry, enzyme-based hybrid organic inorganic nanoflowers are drawing attention in the biocatalysis field due to the development and exploitation altough other strategies and immobilization protocols.It is reported that Surfactant-activated lipase-inorganic hybrid nanoflower (activated hNF-lipase) shows progress on enzymatic performance (Cui and Zhao ,2016).The latest improved activated hNF-lipase shows 460% and 200% higher activity when compared with native lipase and conventional lipaseinorganic hybrid nanoflower (hNF-lipase). In the light of these results, the activated hNF-lipase with higher activities are the promising new alternatives for the industrial

applications such as in the industrial enzyme catalysis. Lee et al. mentioned in their study that prepared glutaraldehyde-treated lipase-inorganic hybrid nanoflowers had been taken adventage of their catalytic performance as immobilized enzymes.

Cobalt chloride as an encapsulating agent is used in the synthesis of protein-inorganic nanohybrids with enhanced catalytic properties .When a comparison is done between advanced nanohybrids and free lipase, nanohybrids exhibited an improved activity (181%), enhanced catalytic properties at higher temperatures, storage stability, and reusability (Kumar et al., 2017) .

With the help of developing technology, the potential of enzyme-based hybrid nanoflowers is exceeded its limit; under the light of this, new point of views on biosensing devices such as biosensors etc. are gained and helps to redefine the applied approximations. The communuties of science and biotechnology are considering the noval developments on biosensing/bioimaging technology. The beneficial effect of newly developed biosensors etc. let them make these considerations. Biosensor is defines as "a device that uses specific biochemical reactions mediated by isolated enzymes, immunosystems, tissues, organelles or whole cells to detect chemical compounds usually by electrical, thermal or optical signals" in IUPAC (International Union of Pure and Applied Chemistry) (IUPAC, 1997) .The main logic of biosensor device is that the recognition process depends on the implementation of biochemical mechanisms. Biosensor, that transform specific biological activity into measurable signal, is a detector device with high presicion (Rasheed et al., 2018) . In a single nanoflower, it is given affinity to two enzyme components; Gox and HRP. This new sensor decreased the diffusion and decomposition of H_2O_2. Also, this sensor improves the sensitivity of glucose detection (Sun et al., 2014). Somturk et al. declares in their article that they synthesized a sensor, copper ion incorporated horseradish perioxide-based hybrid nanoflowers, for detection of dopamine.

In the study of Xu et.al.,L-arabinose isomerase-copper hybrid nanoflowers is handled. It is shown that the production of L-ribulose from L-arabinose is successfully don with a conversion rate of 60% within 2 days . As an another example, Ke et.al. produce lipase-calcium hybrid nanoflowers in order for the chiral resolution of (R,S)-2-pentanol with vinyl acetate as an acyl donor Findings point that high enantioselectivity nearly over 90% is obtained under optimal conditions. It is achieved by nanoflowers' great potential in the industrial field of biocatalytic applications.

Furthermore, amplified catalytic activity of metalloporphyrin-copper hybrid nanoflowers is observed for the catalysation of the cyclohexene epoxidation reaction (He, 2017). Hybrid nanoflowers has been drawing attention for the usage in environmental pollutant treatments, particularly. Moreover, Huang et.al. succeed to decompose organic pollutants e.g. Rhodamine B; 97% of the pollutants are removed in 4 hours. They use BSA-copper hybrid nanoflowers as peroxidase mimetics with a high efficiency rate. In different medium such as; water, hair, food and cigarette, BSA-copper hybrid nanoflowers can be used as strong adsorbents for cadmium and lead ions.

1.5. The Aim of Study

In this study, chemical characterization of Y140H and wild type H-NOX protein from thermophilic bacteria called as *Thermoanaerobacter tencogenesis* (T*t*H-NOX) protein was performed. Mutant T*t*H-NOX protein was created by replacing the thyrosine-140 residue in the heme active pocket whith histidine using site-directed mutagenesis method. This was performed by Joanna Efua AGGREY-FYN in our laboratory who used T*t*H-NOX as scaffold for rational protein design (Aggrey-Fynn and Surmeli, 2018). The catalytic activity towards oxidation of guaiacol and amplex red by the Y140H mutant and wild type protein was be investigated under different kinetic conditions and the kinetic paramaters of ABTS oxidation by Y140H mutant protein was determined. Also stability of T*t*H-NOX proteins in organic solvents were investigated. In addition wild type and mutant proteins were immobilized with a novel and elegant immobilization approach that is used for creating hybrid organic–in organic nanoflowers. This study will contribute to the understanding of heme protein like sGCs and investigate their catalytic potentials.

CHAPTER 2

MATERIAL AND METHOD

2.1. Materials

2.1.1. Vectors Cells Plasmid Kit and Mediums

- Wild Type and Y140H T*t*H-NOX plasmid in pET- 20b obtained from previous study of Joana Efua AGGREY – FYNN
- *E.coli* DH5α competent cells were used for cloning of plazmids . *E.coli* BL21 (DE3) were used for gene expression .
- Presto™ Mini Plasmid Kit were used for plazmid isolation
- LB broth medium (10g/L tryptone, 5g/L yeast extract and 10 g/L NaCl) were used for cell growth .
- Cell growth during the transformation were performed with SOC medium.
- For large scale cell growth Terrific Broth was used.

2.1.2. Chemicals and Equipments

- *Chemicals*: 5-Aminolevulinic acid (ALA), Ampicillin, Isopropyl β-D-1-thiogalactopyranoside (IPTG), Protein Leader, Sodium Dodecyl Sulfate (SDS), Polyacrylamide, HisPur™ Ni-NTA Resin, Hemin, ABTS, Guaiacol, Amplex Red,
- *Equipments*: Centrifuge, Sonicator, Dry-bath, Water-bath, pH Meter, Nanodrop, UV-Vis Spectrophotometer, SEM , EDX spectroscopy.

2.2. T*t*H-NOX Expression Plasmid Transformation, Purification and Sequence Conformation

The Pet 20b plasmids from previous study in our laboratory (Aggrey-Fynn and Surmeli, 2018) that containing the Wild type and mutant Y140H T*t*H-NOX gene sequences together with C-terminal histidine tag were transformed into competent DH5α cells with heat shock transformation method. The transformed plasmid were incubated on ampicillin-LB-agar plates at 37℃ overnight.

For plasmid isolation, selected DH5α colonies were cultured under sterile conditions in 5 ml LB media with 100 mg/ml ampicillin for both colony. The plasmids were then isolated using the Presto™ Mini Plasmid Kit which was designed for plasmid DNA purification. Approximately 50 µl pure plasmid were isolated for each sequence. NanoDrop Spectrophotometer was used to determine the concentration and purity of plasmids. Then the prufied plasmids were sent to Triogen Biotechnology to confirm the accuracy of the sequences. The sequences were confirmed with the GENEIOUS sequence alignment program.

To examine protein expression, wild type and mutant plasmids were transferred into expression vector, competent BL21 (DE3) and grown in LB plates containing 50 mg / ml apicillin. Selected colonies were incubated overnight at 37 ℃ in LB broth.

2.3. Expression of Wild Type and Mutant Y140H T*t*H-NOX Proteins

10 ml of LB media containing 100 µg/ml of ampicillin were inoculated with 100 µl of cell culture that incubated overnight. Then these were grown until the absorbances at 600 nm (OD_{600}) were in the range of 0.5-0.6. When absorbances reach the desired range 1 ml of the cells were collected and named was T= 0 and pelleted to remove supernant .

Then they were frozen at -80℃. Isopropyl β-D-1-thiogalactopyranoside (IPTG) solutions which a final concentration of 0.5 mM were added to both culture to induce expression. Incubation was continued for 1 more hour at 37 ℃ and 220 rpm. The OD_{600} after 1 hour was measured and named as T = 1. Normalization was performed by taking

the absorbance measurements as reference. Cells were pelleted and stored at -80℃. The temperature was reduced to 25 ℃ and the incubation was continued overnight at 220 rpm. When the time was completed, the OD_{600} was measured and normalized to the absorbance values then pelleted and stored at -80℃.

2.4. SDS-PAGE Analysis

Sodium Dodecyl Sulfate Polyacrylamide Gel Electrophoresis (SDS-PAGE) was utilized to examine the success of T*t*H-NOX proteins expressions according to their molecular weight throughout the study. For this purpose, the pelleted cells from the small scale protein expression analysis were prepped with SDS loading dye and 1 mM dithiothretiol (DTT). The samples were loaded into polyacrylamide gel after being heated to 90 ℃. SDS denatured and applied the negative charge on the proteins make them linear. DTT decreased the sulfide bonds in the protein structure consequently unfolding the structures of the proteins.

The linear, negatively caharged proteins were separated based on their molecular weights trough the electric field which is supplied through the gel. Protein that have higher molecular weight moved slower than the low weighted ones. To determined the protein sample size Thermo Scientific Unstained Protein Molecular Weight Marker which has a mixture of seven purified proteins ranging from 14.4 kDa to 116 kDa was used.

2.5. Isolation and Purification of Wild Type and Mutant Y140H T*t*H-NOX Proteins

2.5.1. Large Scale Expression

To obtain big amount of Wild type and mutant proteins 2 L protein expression assay were employed. From the glycerol stocks of WT and mutant Y140H T*t*H-NOX, 10 ml overnight cultures of TtH-NOXs were prepared in sterile ampicillin - LB broths. 2 L autoclaved terrific broths which contain 0,1 mg/ml ampicillin were inoculated with 5 ml

overnight cultures. Until OD_{600} were about 0,8 they were grown at 37℃. Expression and heme biosynthesis were induced by adding of 0,1 mM IPTG and 0,5 mM 5-aminolevulinic acid hydrochloride (ALA), incubations were contiuned overnight at 25℃. ALA was used to increase the heme synthesis and heme protein production efficiency. The cells were harvested with centrifuge at 3200 rpm , 10℃ for 30 minutes. Pelleted cells were stored at -80℃ for isolation and prufication steps.

2.5.2 Protein Extraction

Protein extraction and purification of WT and mutant T*t*H-NOX were performed with the Gravity - Flow Column with HisPur Ni-NTA resin using with three buffers shown in Table 2.1. Firstly the weight of cell pellets determined after that Lysis Buffer added to cells in a 1:1 (mass : volume) ratio. The dissolved cell lysates sonicated on ice with interval of 1 minute for an avarage of 7 cycles. Sonication step were performed until a water consistency was achived. Cell lysates were heated for 40 minutes at 70 ℃ after that pelleted at 3200 rpm at 10℃ for 2 hours.

Buffers	Triethanolamine (mM)	Imidazole (mM)	Sodium Chloride (mM)	Benzamidine Hydrochloride (mM)	Phenylmethylsulfonyl Fluoride (mM)
Lysis Buffer	50	10	300	1.34	0.2
Elution Buffer	50	150	300	-	-
Dialysis Buffer	50	-	20 with 5 % glycerol	-	-

Table 2.1. Bufers for T*t*H-NOX isolation and purification.

2.5.3. Protein Purification through Affinity Chromatography

1 ml Nickel -NTA resin (Thermo Scientific) was settled in column with the protocol that was provided from Thermo Scientific. The settled resin was equilibrated with 5 -10 ml of Lysis buffer. Supernatants obtained after centrifugation were added to the column. In this type of purification T*t*H-NOX protein which has C-terminal His-tag binds to the resin. Due to low imidazole concentration of Lysis buffer, proteins that have weak bind through leaving the column. The tigher bound ones remain in the column. After the flow through samples were collected , column was washed with 25 - 30 volumes of Lysis buffer until the wavelength at 280 nm was stable . Then elution was performed in 1 ml aliquots with Elution buffer which has high imidazole concentration. To remove imidazole and undesired small compounds, eluted fractions were desalted using by PD-10 Desalting Columns which containing Sephadex™ G-25 Medium (GE Healthcare) . Eluted fractions were added to the desalting column which equlibrated with 10-15 volumes of Desalting buffer. Desalting was performed in 1 ml aliquots with desalting buffer. Purifed proteins were concentrated in 6 ml Pierce™ Protein Concentrator PES, 3K MWCO (Thermo Scientific) concentration tubes until a volume of about 800 µl. 50 µl aliquots were prapared and stored at - 80°C .

To confirm the efficiency of isolation and prufication, SDS PAGE analyses were performed using 10 µl samples which were collected at every step of the isolation and prufication processes.

2.6. Heme Reconstitution of WT T*t*H-NOX protein with Hemin

Reconstitution of Apo T*t*H-NOX protein was performed with Hemin that provided from Sigma Aldrich. Hemin was dissolved in 0.1 M NaOH. For each 1 µM apoprotein 4 µM hemins were added and the apoproteins were incubated overnight at +4 °C on ice with 100 mM potassium phosphate pH 7 buffer. Removing of the excess hemin and salts was performed with PD-10 Desalting Columns which containing Sephadex™ G-25 Medium (GE Healthcare). In the column equlibration and desalting process a Desalting buffer which containing 100 mM Kpi ,20 mM NaCl and 5% glycerol, pH 7

were used. After purification step, reconstituted T*t*H-NOX protein was concentrated with Amicon® Ultra 15 mL Centrifugal (Merck) concentration tubes until a volume of about 1 ml.

2.7. Ultraviolet-Visible (UV-Vis) Spectrophotometric Analysis

In order to determine the UV spectroscopic characteristics of the Wild type and Mutant T*t*H-NOX, 70 X dilutions using Desalting Buffer were prepared and the absorbance measurements 650-250 nm were taken. This large wavelength includes the α/β peaks for protein structure, the heme peak or Soret peak which is a peak in the blue region of visible spectrum and ranges around 400 nm, and the protein peak at 280 nm. Unique characteristics of wild type and T*t*H-NOX Y140H were observed through their Soret and α/β peaks. were investigated

2.8. Catalytic Analysis

To investigate chemical and enzymatic properties of wild type and mutant T*t*H-NOXs, guaiacol and amplex red oxidation were performed. Addition to these, oxidation of ABTS by Y140H was investigated. In all protocols, protein, substrate reagent concentrations and measurement analyses were obtained from literature.

2.8.1. Catalytic Oxidation of Guaiacol

To invastigate the catalytic performance of T*t*H-NOX proteins guaiacol oxidation which is widely used colorimetric assay was chosen among the known peroxidase-catalayzed rection. Three control kinetic experiments were set up with 3 µM for each WT and Y140H T*t*H-NOXs according to Table 2.2.

Control Experiments	H_2O_2 Concentrations (mM)	Guaiacol Concentrations (mM)	pH of 50 mM Potassium Phosphate Buffer
1	0.025,0.1,0.25,0.5 and 1	5	7.5
2	1	1,1.5,2.5,3,5 and 7	7.5
3	1	5	5.8,6.8,7.5 and 8.0
4 (No Protein)	1	5	7.5
5 (No H_2O_2)	-	5	7.5

Table 2.2. Control experiment set up for Guaiacol oxidation assay.

Using these setup, the tetraguaiacol formation was followed at 470 nm every 0.5s for 25 minutes. The spectroscopic characteristics and kinetic paramaters were measured for each Y140H mutant and comparisons were made with the wild type and negative controls.

2.8.2. Catalytic Oxidation of Amplex Red

In the presence of H_2O_2 , amplex red can be oxidized by the peroxidases and the red-fluorescent oxidation product resorufin is produced. Investigation of amplex red oxidation catalyzed by T*t*H-NOX protein was performed with 1.5µM enzyme and 10 µM Amplex red in the presence of 1.5 mM H_2O_2 at pH 7.5 (50 mM potassium phosphate). Formation of resorufin was followed at 570 nm at room temperature. At different H_2O_2 concentrations kinetic parameters were investigated with WT and Y140H mutant.

2.8.3. Catalytic Oxidation of ABTS by T*t*H-NOX Y140H

The one-electron oxidation of ABTS into the green radical cation, $ABTS^{\bullet+}$ was performed with 0.5 µM mutant T*t*H-NOX enzyme in the presence of 1 mM ABTS and 1mM H_2O_2 at pH 7.5 (50 mM potassium phosphate). $ABTS^{\bullet+}$ formation was monitored at 736 nm at room temperature. Kinetic parameters were investigated at different ABTS concentration for Y140H mutant.

2.9. Synthesis of copper ion incorporated T*t*H-NOX-based hybrid nanoflowers

T*t*H-NOX - Cu^{2+} Hybrid Nanoflowers synthesis was performed using T*t*H-NOX proteins as organic part and Cu (II) ions as inorganic part (Somtürk et al. 2015). For this purpose, firstly, Cu (II) ion (120 mM), PBS (10 mM; pH 6-9) and enzyme stock (1 mg / mL) solutions were prepared.

Then, 333 µL of Cu (II) ion solution was added to the PBS solution in a certain volume in 50 mL falcon tubes. The mixture was vortexed vigorously for 30 seconds. Then, the enzyme stock solution was added to this mixture in a final concentration of 0.02 mg / mL protein in medium and vortexed vigorously for 30 seconds. The resulting mixture was incubated for 3 days. Hybrid nanoflower synthesized after incubation was centrifuged. The supernatant obtained after centrifugation was separated for protein determination. The cottage cheese was washed at least three times and allowed to dry.

2.10. Investigation of T*t*H-NOX proteins stability at different organic solvents

Investigation of T*t*H-NOX proteins stability were performed with methanol, ethanol and acetonitrile. Amplex Red peroxidation reactions were performed with 1.5 µM TtH-NOX proteins with 10 µM Amplex Red and 1mM H_2O_2 in the presence of 2.5 %

and 5% organic solvent at pH 7.5 (50 mM potassium phosphate). Production of resorufin was analyzed by monitoring fluorescence emission (570 nm excitation and 585 nm emission) at 570 nm.

CHAPTER 3

RESULTS AND DISCUSSIONS

3.1. WT and Mutant T*t*H-NOX Expression Plasmid Transformation, Purification and Sequence Conformation

The Pet 20b plasmids from previous study in our laboratory (Aggrey-Fynn and Surmeli, 2018) that containing the Wild type and mutant Y140H T*t*H-NOX gene sequences were transformed into competent DH5α cells by the heat-shock technique. Each of cloned plasmids were purified through the Presto™ Mini Plasmid Kit and their concentrations were measured by the the NanoDrop Spectrophotometer. Concentration of purified Wild type and Y140H T*t*H-NOX were measured 205.88 ng/µl and 241.04 ng/µl.

Each plasmid were sequencing by the Triogen Biotechnology company. Sequence of plasmids were confirmed through the GENEIOUS program. Then each plasmid were transformed into BL21 (DE3) compotent *E.coli* cells for protein expression. The amino acid sequences are shown in appendix.

3.2. Expression of WT and T*t*H-NOX Y140H Proteins

Overnight cultures of WT and T*t*H-NOX Y140H colonies were prepared and through the 0.5 mM IPTG the protein expression was induced where the OD_{600} was reached the 0,7. After 1h cells were harvested. To observe the protein expression SDS PAGE analysis was performed. Glycerol stocks were prepared for the samples with T*t*H-NOX expression.

3.2.1. Expression of WT T*t*H-NOX

SDS PAGE analysis showed for protein expression after one-hour expression induction with as shown in Figure 3.1. Samples were taken before induction with IPTG (t=0) and 1 hour after induction (t=1). Protein expression band was observed at 23 kDa that is the MW of WT T*t*H-NOX protein.

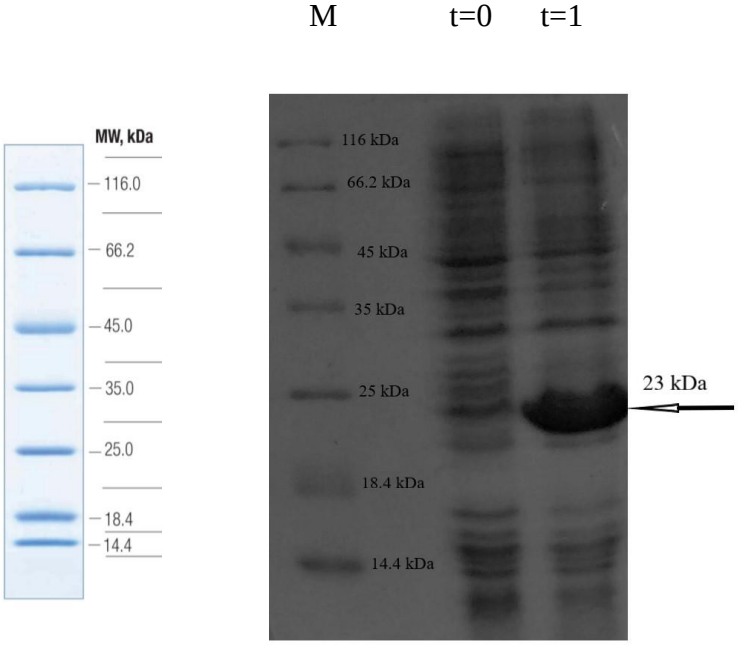

Figure 3.1. Protein expression band for WT TtH-NOX (23.215 kDa). M: Protein molecular weight marker t=0 indicates control sample before IPTG induction and t=1 indicates sample which was taken one-hour after IPTG induction.

3.2.2. Expression of T*t*H-NOX Y140H

SDS PAGE analysis of T*t*H-NOX Y140H showed for protein expression after one-hour expression induction with IPTG. Protein expression band was observed at 23kDa that is the MW of Y140H T*t*H-NOX protein.and results was shown in Figure 3.2.

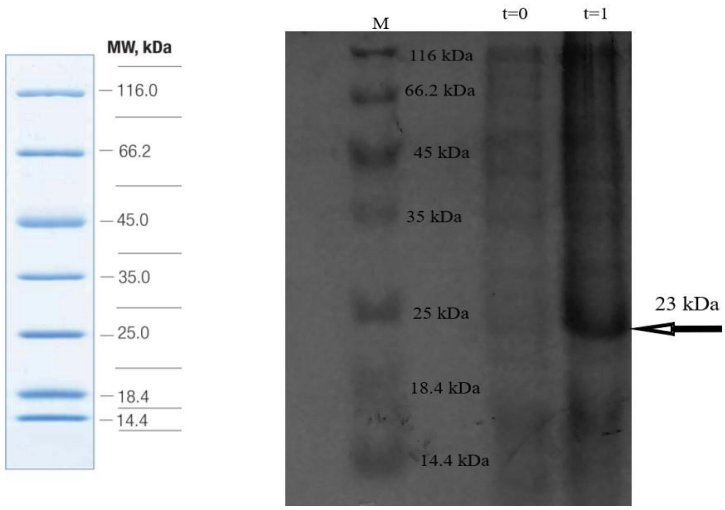

Figure 3.2. Protein expression band for Y140H T*t*H-NOX (23.189 kDa). M: Protein molecular weight marker t=0 indicates control sample before IPTG induction and t=1 indicates sample which was taken one-hour after IPTG induction

3.3. Extraction and Purification of T*t*H-NOX Proteins

To obtain big amount of wild type and Y140H mutant T*t*H-NOX proteins, protein expressions were performed at large scale as described in 2.5.1. section of the Methodology. Then proteins were isolated by affinity chromatography method, the Gravitiy-flow Column with HisPur Ni-NTA Resin, as described in 2.5.3. Method section. Removal of excess imidazole was performed with desalting column. Sample fractions were collected from isolation and purification steps to made SDS PAGE analysis.

3.3.1. Isolation and Prufication of Wild Type T*t*H-NOX

From 2 L cell culture of wild type T*t*H-NOX expressing *E.coli* BL21(DE3) approximately 8.5 g pellet was harvested. End of the purification, the final concentration of protein was determined as 586 µM. The final yield of the protein was determined about 5.86 mg from 2L. In Figure 3.3. SDS PAGE analysis of WT T*t*H-NOX purification steps was shown, protein bands were observed about 23 kDa.

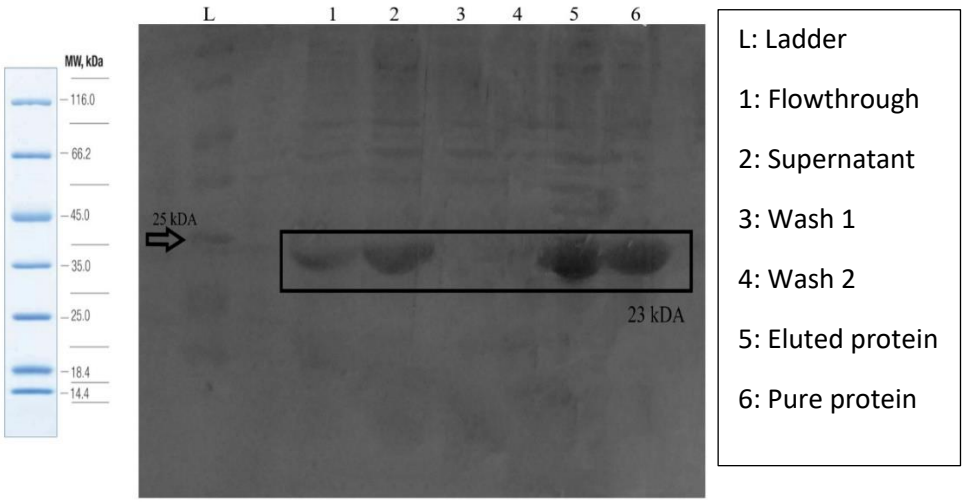

Figure 3.3. SDS PAGE showing purification steps of WT T*t*H-NOX. L: Ladder, 1: Flowthrough, 2: Supernatant, 3: Wash 1, 4: Wash 2, 5: Eluted protein, 6:Pure protein

3.3.2. Isolation and Purification of T*t*H-NOX Y140H

Approximately 11.7 g pellet was harvested after 2 L large scale expression of Y140H mutant. End of the purification the final concentration of protein was determined as 500 µM The final yield of the protein was determined about 10 mg from 2L. SDS PAGE analysis of samples taken from each purification step is shown in Figure 3.4.

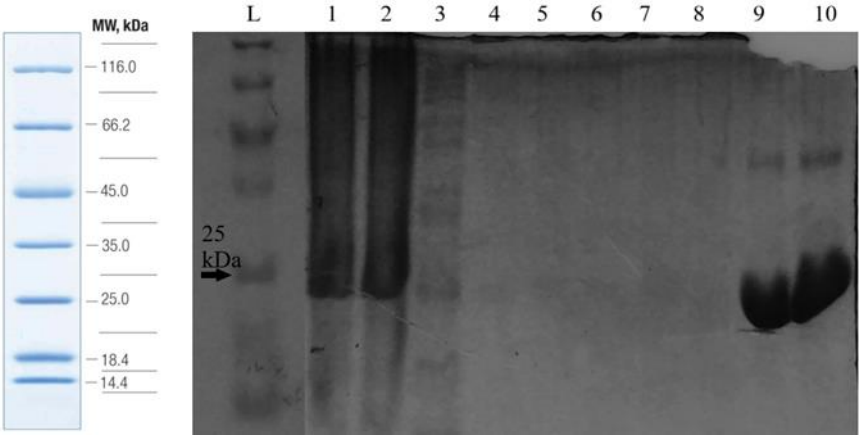

Figure 3.4. SDS PAGE showing purification steps of Y140H T*t*H-NOX. Last two protein bands were about 23 kDa. L: Ladder, 1: Cell lysate, 2: Pellet, 3: Supernatant, 4: Flowtrough, 5:Wash1, 6: Wash 2, 7: Wash 3, 8: Wash 4, 9:Eluted protein,10: Pure protein

3.4. Spectrophotometric Analysis of Purified T*t*H-NOXs

To investigate spectroscopic characteristics of T*t*H-NOX proteins, the absorbance measurements from A_{700} to A_{250} of the isolated proteins were performed in to 50 mM TEA, 20 mM NaCl, and 5% glycerol. The measurement of T*t*H-NOX Y140H show the Soret peak,which is an intense at the maximum wavelength for heme absorption, at 410 nm the same as that found in literature, in Y140H mutation, changing of the netural tyrosine with a positively charged histidine caused alteration in distal pocket electronic charge and this is resulted with the shift in Soret (Aggrey-Fynn and Surmeli, 2018).The alpha/beta bands of protein was observed at 587/547 nm respectively. Due to tyrosine and tryptophan residues a peak observed at 280 nm (Figure 3.5. b). As seen in Figure 3.5.a, wild type T*t*H-NOX shown an intense peak at 280 nm. However the Soret peak of wild type protein was very low. It was concluded that almost all of the purified protein was in the form of apoprotein. To overcome this problem, heme reconstitution was performed and described in 2.6. Method section.

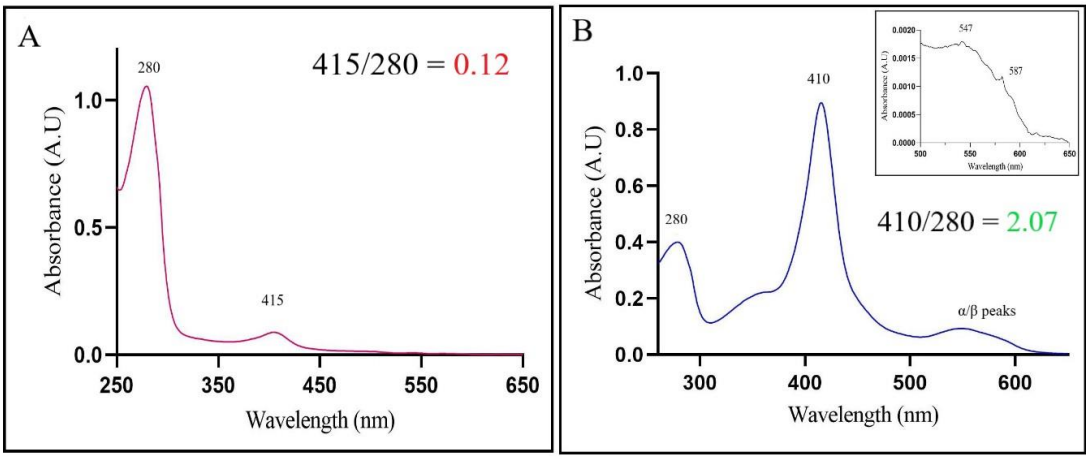

Figure 3.5. The UV-Vis spectra of T*t*H-NOXs. (A) The UV-Vis spectra of WT T*t*H-NOX as isolated. (B) The UV-Vis spectra of T*t*H-NOX Y140H as isolated, inset α/β peaks.

3.5. Heme Reconstitution of WT T*t*H-NOX

Heme binding of heme renconstituted wild type protein was investigated with taken UV spectra measurement. Spectra was taken the absorbance measurements from A_{700} to A_{250} of the isolated proteins were performed in to 100 mM potassium phosphate buffer, 20 mM NaCl and 5% glycerol. In the UV spectra taken before heme reconstitution that 280 nm to Soret absorbance ratio (415/280) was observed as 0.12 (Figure 3.6.a).It was conculeded that the form of WT T*t*H-NOX was apo.

After heme reconstitution, a soret peak and α/β bands was observed at 415 nm and 589/552 nm. After the heme reconstitution process 280 nm to Soret absorbance ratio (415/280) was observed as 1.5 as seen in Figure 3.6.b. Thus the holo form of WT T*t*H-NOX protein was obtained succsessfuly.

3.6. Identification of The Oxidation State of Heme Iron

The investigation of the oxidation state of Heme iron were performed with cyanide binding experiments. Cyanide binding to ferric hemoproteins causes the changes in the UV spectrum. Furthermore, cyanide binding to ferric T*t*H-NOX results in a shift in Soret absorbance from 415 to 420nm (Dai and Boon, 2010).

The soret peak for mutant protein is the same as which found in literature , ferric state (Fe^{+3}) . In the presence of KCN soret absorbance of Y140H, a significant shift from 410 nm to 421 nm (Figure 3.7.b). Through addition of increasing amount of KCN the soret absorbance shift to 419 nm. It is possible the say that heme reconstituted wild type T*t*H-NOX at ferric state (Fe^{+3}) (Figure 3.7.a).

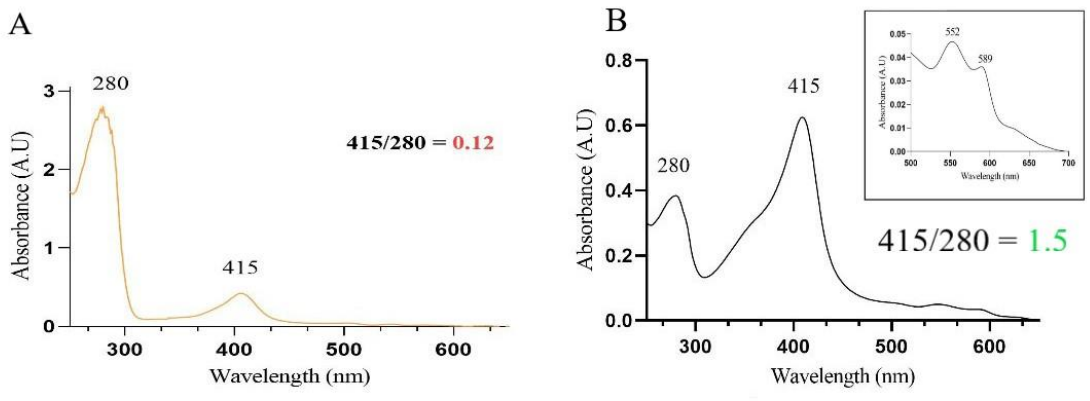

Figure 3.6. The UV-Vis spectra of WT T*t*H-NOX taken before (A) and after (B) heme reconstution.

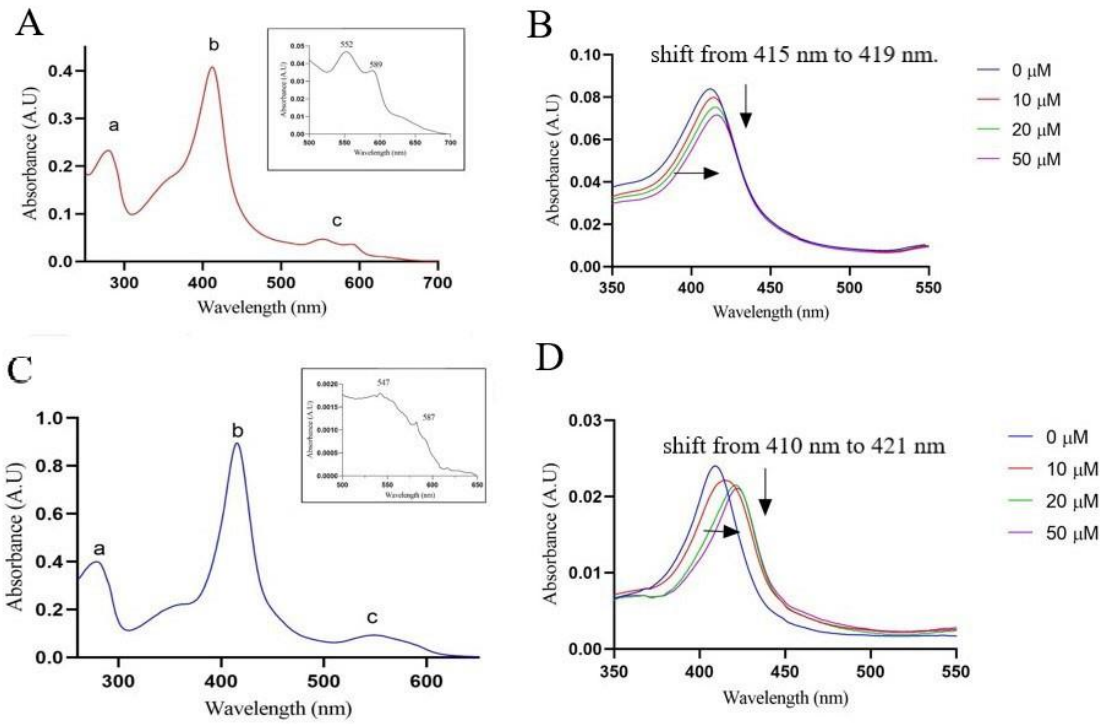

Figure 3.7. Identification of The Oxidation State of Heme Iron. (A) UV-Vis spectra of WT T*t*H-NOX after Heme Reconstitution as isolated and (B) in the presence of 0-50 µM KCN in phosphate buffer (50mM) a pH 7.5 at 25°C. (C) UV-Vis spectra of T*t*H-NOX Y140H as isolated and (D) in the presence of 0-50 µM KCN in phosphate buffer (50mM) a pH 7.5 at 25°C.

3.7. SEM and EDX Analysis of copper ion incorporated T*t*H-NOX-based hybrid nanoflowers

Nanoflowers were synthesized at the Özdemir Laboratory at the University of Erciyes (Kayseri, Turkey). These hNFs contain three major components: phosphate ions from the PBS solution, Cu^{2+} ions and T*t*H-NOX enzyme. The possible formation mechanism of copper ion incorporated T*t*H-NOX-based hybrid nanoflowers were occurred in three steps. In first step, which is called nucleation, initiation the nucleation of nanocrystals are made by the favorably coordination with copper phosphate and the amine groups in the backbone of T*t*H-NOX (Somturk and Özdemir, 2015). Second step is growth, at this process enzyme acts like an adhesive. Primary nanocrystals are combined with T*t*H-NOX enzyme to alike flower petals, on copper phosphate nanocrystals (Somturk and Özdemir, 2015). Final step named as formation is that the nanocrystals growing kinetically and hierarchically complete the growth by saturating (Somturk and Özdemir, 2015). As a consequence, the T*t*H-NOX hNFs are efficiently produce at the end of the anisotropic growth process.

Formation of copper ion incorporated T*t*H-NOX-based hybrid nanoflowers were investigated at different pH values which is above and below isoelectronic point of T*t*H-NOX. The isoelectric point (pI) refers the value where a protein expected to be neutral. Above this point, the protein is expected to be negatively charged, while below this point it is thought to be positively charged.

Isoelectric point of T*t*H-NOX (pI) is 8.6. Theoretically expected that at the pH values below the pI , the T*t*H-NOX molecules predominately protonated and positively charged. At this situation due to the presence of Cu^{2+} cations, very strong repulsions will result between them. For this reason, formation of T*t*H-NOX hNFs will not be occurred. However, formation of T*t*H-NOX hNFs was achieved at pH 5 through the pH 9 as shown in the SEM images presented in Figure 3.8, it was observed that the nanoflowers take a *hortensia*-like shape. Analysis of the elemental composition of T*t*H-NOX hNFs was performed with energy-dispersive X-ray (EDX) technique. As seen in the peaks of EDX spectrum at the figure 3.9, demonstrative elements were observed Cu, P and O which are came from $Cu_3(PO_4)_2$ nano crystal structures while N and C that came from the T*t*H-NOX enzyme. Formation of T*t*H-NOX hNFs and encapsulation of the T*t*H-NOX was

confirmed through this result. Addition to this, homogeneously distribution of Cu, C, N, O and P elements in hNF structures were confirmed with SEM element mapping analysis. (Figure 3.10)

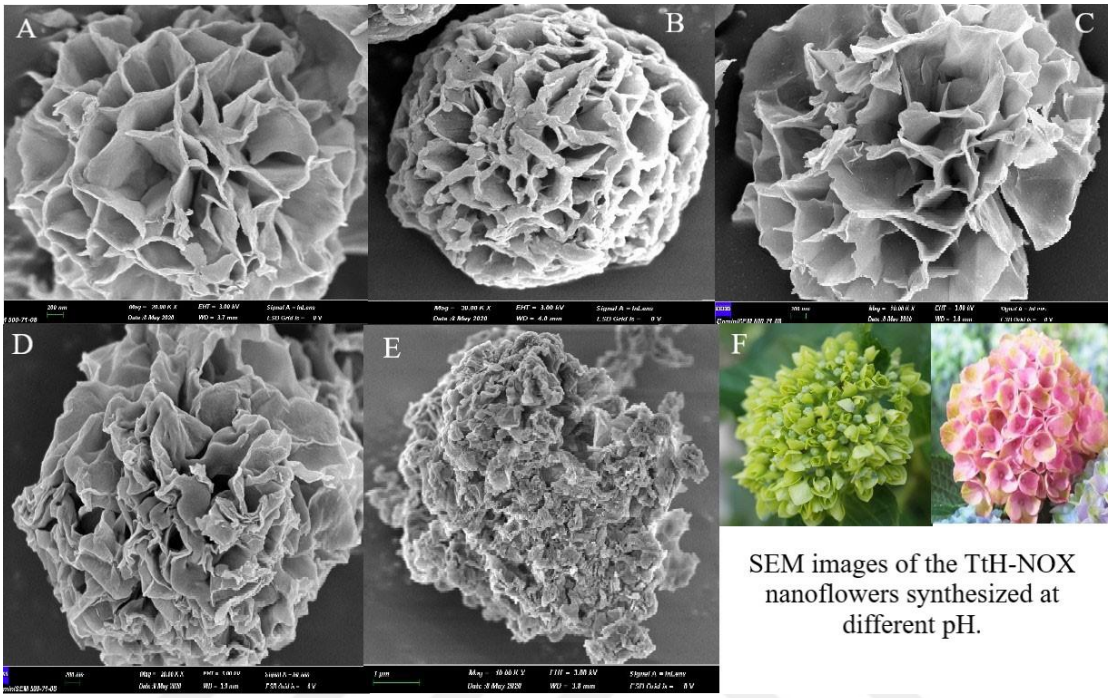

Figure 3.8. Formation of the T*t*H-NOX hNFs at different pH values. (A) pH 6, (B) pH 5, and (C) pH 7, (D) pH 8 and (E) pH 9 . (F) Images of *hortensia* flower.

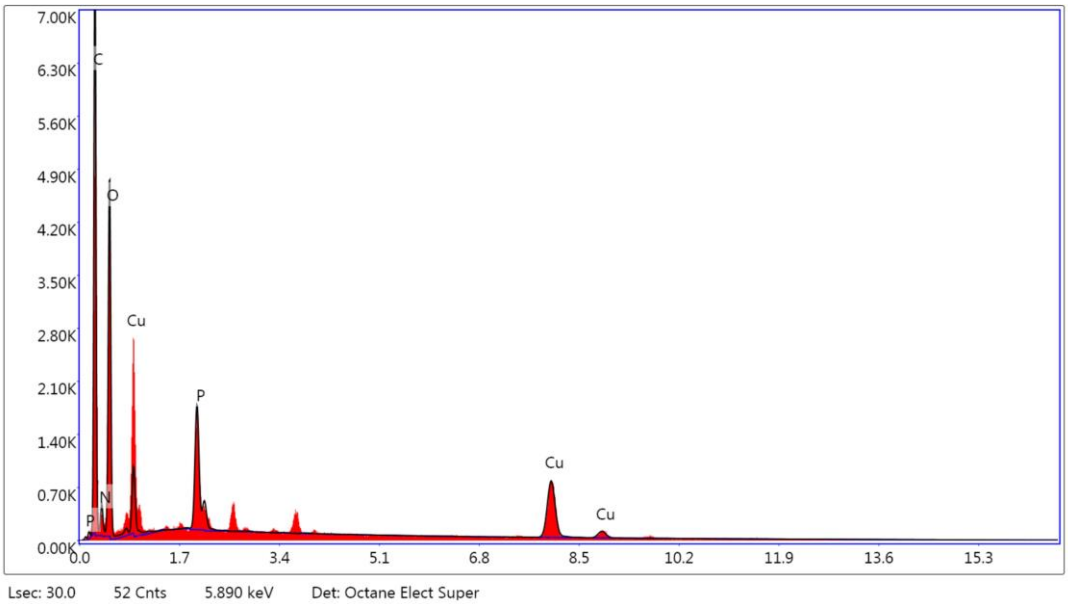

Figure 3.9. EDX analysis of the T*t*H-NOX hNFs. Cu, P and O peaks came from $Cu_3(PO_4)_2$ nano crystal, N and C came from T*t*H-NOX enzyme.

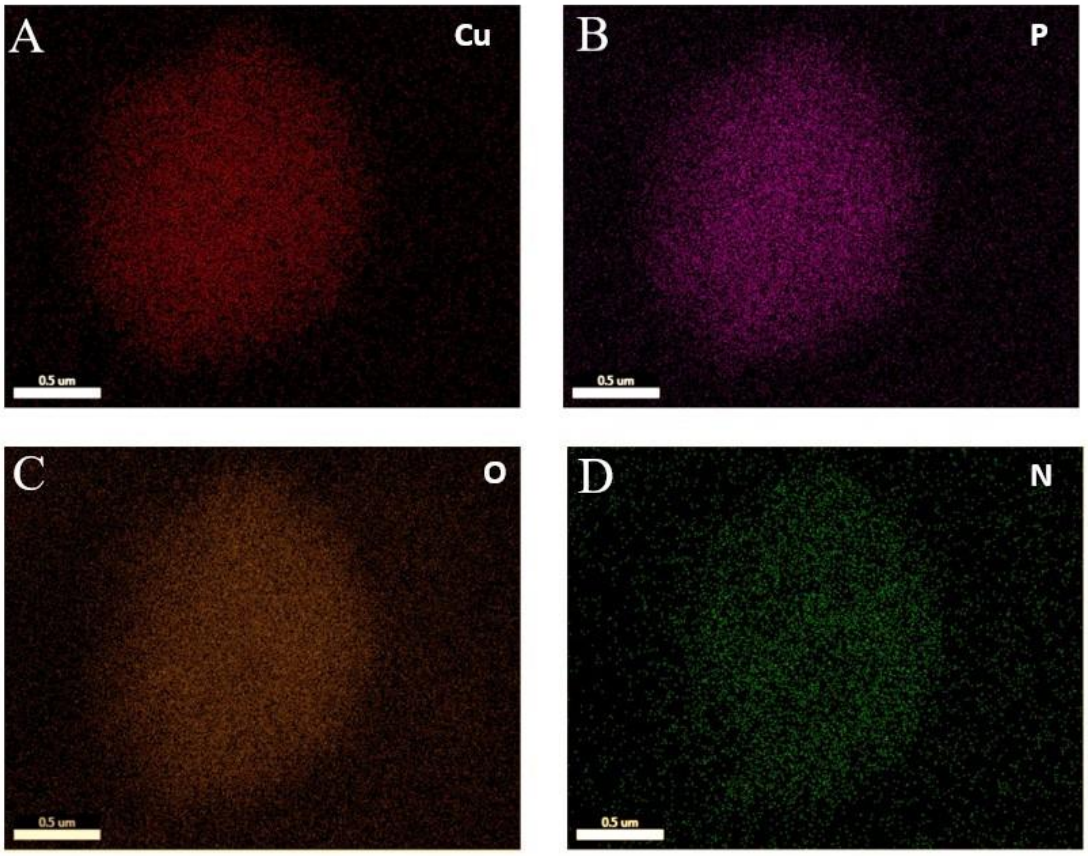

Figure 3.10. SEM element mapping analysis of T*t*H-NOX hNFs. (A) Cu, (B) P, (C) O and (D) N. These elements were disturbed in T*t*H-NOX hNFs homogeneously.

3.8. Chemical Characterizations of T*t*H-NOX Proteins

3.8.1. Oxidation of Guaiacol

Peroxidases are hemeproteins which can catalyze the oxidation of a substrates like guaiacol or ABTS to cation and tetraguaiacol (Guo et al.,2012). To investigate and compare the peroxidase activity of Wild type T*t*H-NOX and T*t*H-NOX Y140H, the oxidation of the guaiacol to tetraguaiacol which has a characteristic amber colored product formed from guaiacol and absorbance maximum of 470 nm, as seen in the equation 1, was following in the presence of H_2O_2.

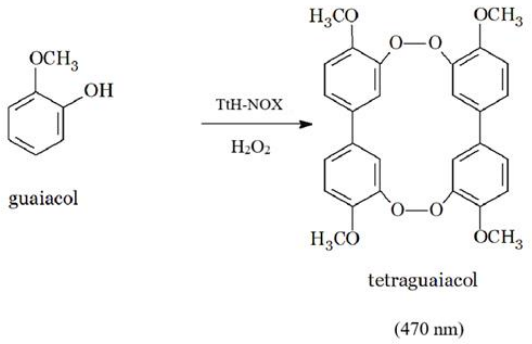

(1)

3.8.1.1. Catalyic activity of WT T*t*H-NOX towards Guaiacol Oxidation

Oxidation of 5 mM guaiacol catalyzed by 5 µM WT TtH-NOX presence of 1 mM H_2O_2 in phosphate buffer at pH 7.5 and 25 °C. As seen in figure 3.13, the spectra were taken at 0,2,5,10,20,25,30 and 40 minutes. The spectra showed increase at 415 nm and the formation of a broad band at 470 nm (Figure 3.11.a), indicative of tetraguaiacol formation (Chance and Maehly, 1955). The reaction was completed in 20 minutes and formation absorbance of tetraguaiacol increase with time (Figure 3.11.b).

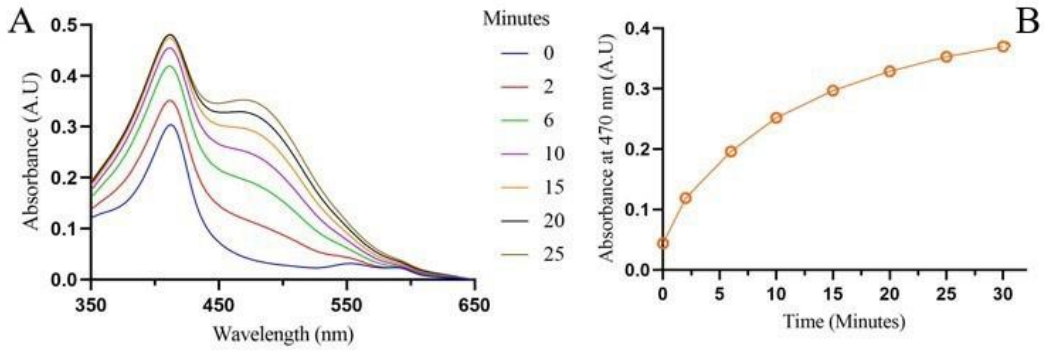

Figure 3.11. (A) Oxidation of guaiacol by H_2O_2 catalyzed by WT T*t*H-NOX. H_2O_2 (1mM) was added to WT T*t*H-NOX (3 µM) and Guaiacol (5 mM) in phosphate buffer (50 mM) at pH 7.5 and 25 °C. (B) getraguaiacol formation at 470 nm with time.

3.8.1.2. Catalyic activity of T*t*H-NOX Y140H towards Guaiacol Oxidation

5mM guaiacol oxidized by 3µM T*t*H-NOX Y140H in presence of 1 mM H_2O_2. As seen Figure 3.12.a, tetraguaiacol formation was observed with abroad band at 470 nm. During the reaction, absorbance at 470 nm was increased whilst the soret peak at 410 nm was increased during the first 20 minutes, then decreased and started to flatten (Figure 3.12.a) As seen in Figure 3.12.b the reaction was completed in 10 minutes and formation absorbance of tetraguaiacol increase with time.

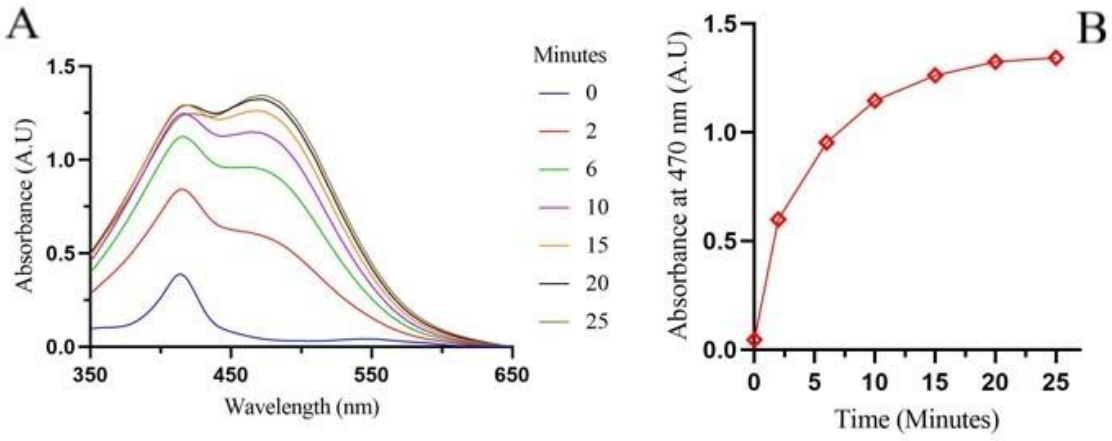

Figure 3.12. (A) Oxidation of guaiacol by H_2O_2 catalyzed by Y140H mutant. 1mM H_2O_2 was added to Y140H mutant (3 µM) and Guaiacol (5 mM) in phosphate buffer (50 mM) at pH 7.5 and 25 °C. (B) tetraguaiacol formation at 470 nm with time.

3.8.1.3. Catalyic activity of WT T*t*H-NOX with Guaiacol

Investigation of guaiacol reaction was performed with three different kinetic experiments. These experiment setups consist of varying concentration of guaiacol, H_2O_2 and at different pHs. In each experiment, the tetraguaiacol formation was followed by increase in absorbance at 470 nm that the maximum absorption of the tetraguaiacol.

3µM of wild type protein was used for each experiment and the absorbance measurements for the kinetic experiments were taken every 0.5 second for 25 minutes.

First kinetic experiments were performed under different guaiacol concentrations (1-7 mM) with 3µM wild type protein in presence 1 mM H_2O_2. As seen in Figure 3.13b, the initial rate of 2.5 mM guaiacol assay was the highest (Figure 3.12.b).

The second set of experiments were performed using different H_2O_2 concentrations of 0 (control), 0.025,0.1,0.25,0.5 and 1 mM in the presence of 5mM guaiacol and 3 µM wild type T*t*H-NOX at pH 7.5. The control experiment (0 mM H_2O_2) was resulted no measurable catalytic activity so, demonstrated that the wild type enzyme only catalyzes the oxidation reaction in the presence of H_2O_2. As seen in Figure 3.14.b, the assay with the highest H_2O_2 concentration (1 mM) showed the highest activity. It is concluded that enzyme efficiency varying with H_2O_2 concentration.

The last set of kinetic experiments were performed with different pH ranges at 5.8, 6.8, 7.5 and 8.0 with 5 mM guaiacol and 1 mM H_2O_2. As seen in Figure 3.15.b, the highets rate was observed at pH 5.8 . This result determined that at least one ionizing group in the active site affects the oxidation reaction rate so, the rate of oxidation is maximum when this group is in the protonated form (Aggrey-Fynn and Surmeli, 2018; Khan et al., 1998). It is possible to concluded that an acid/base catalyst, like peroxidases, may play a role in the peroxidase activity (Aggrey-Fynn and Surmeli, 2018). Also, this result showed a similar ph profile for cytochrome c-550 for oxidation of guaiacol (Diederix et al., 2001). The little absorbance ripples seen in the curve are caused by the unimportant calibration losses caused by the long operating lamp of the UV spectrophotometer. This situation does not affect the accuracy of the results.

The three kinetic experiments for the wild type were all performed in duplicates and results showed that efficiency of WT enzyme depends on pH and H_2O_2 concentration and guaiacol concentration .

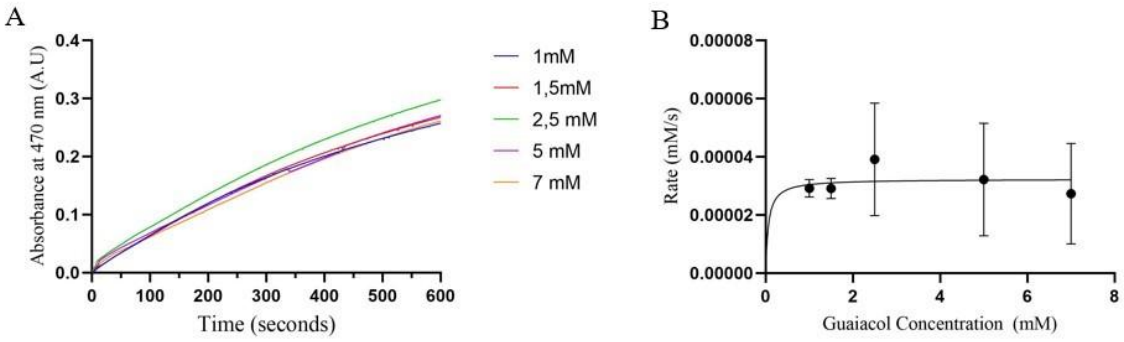

Figure 3.13. (A) Kinetic reactions of WT T*t*H-NOX at different guaiacol concentrations. (B) Rates of reactions. All kinetic experiments were performed at 25°C between 3 µM WT T*t*H-NOX and 1 mM H_2O_2 at pH 7.5.

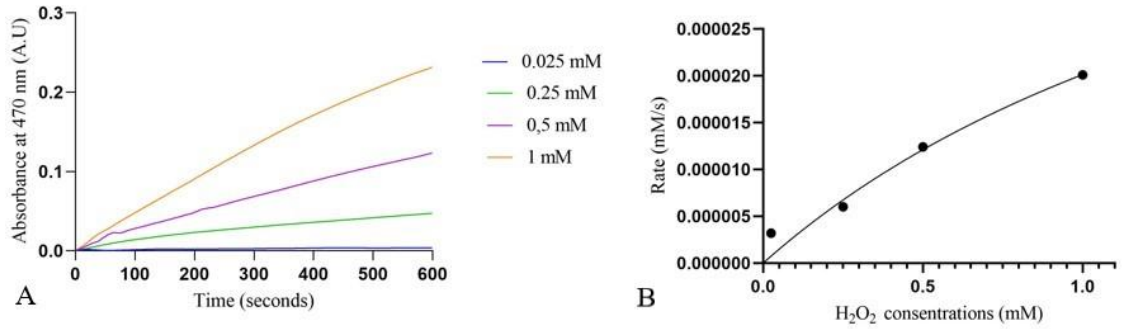

Figure 3.14. (A) Kinetic reactions of WT T*t*H-NOX at 470 nm with different H_2O_2 concentrations. (B) Rates of reactions were performed at 25°C between 3 µM WT T*t*H-NOX and 5 mM Guaiacol at pH

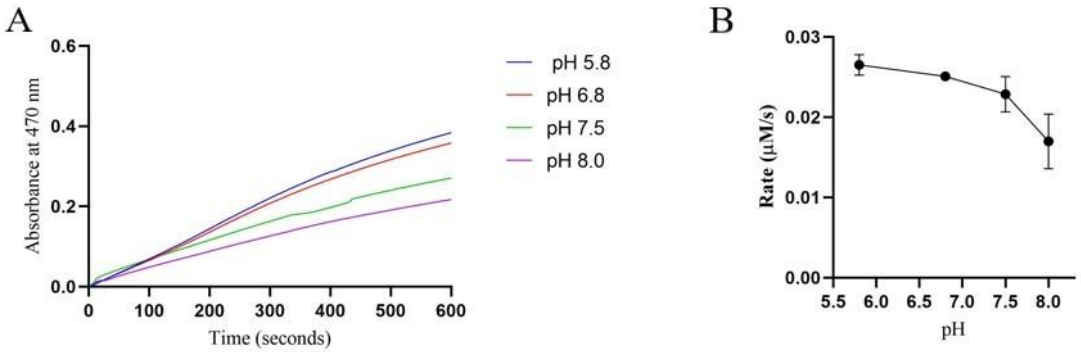

Figure 3.15. (A) Kinetic reactions of WT T*t*H-NOX at 470 nm with different pH ranges. (B) The initial rates of reactions were performed at 25°C between 3 µM WT T*t*H-NOX and 5 mM Guaiacol in presence of 1 mM H_2O_2.

3.8.1.4. Catalyic activity of T*t*H-NOX Y140H with Guaiacol

The T*t*H-NOX Y140H and H_2O_2 oxidized guaiacol in aqueous solution. However, since the catalysis of guaiacol oxidation was never been tested before on T*t*H-NOX Y140H, reaction kinetics investigated with three different kinetic experiments

First of all kinetic experiments were carried out in different guaiacol concentrations (1-7 mM) with 3µM Mutant protein. As seen in Figure 3.16.b, the highest rate was observed at 5mM guaiacol concentrartion.

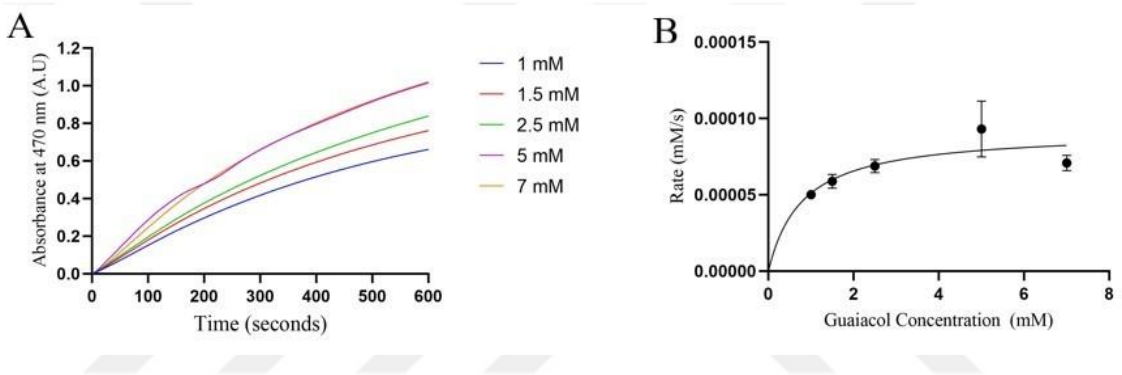

Figure 3.16. (A) Kinetic reactions of T*t*H-NOX Y140H at 470 nm with different guaiacol concentrations. (B) Rates of reactions were performed at 25°C between 3 µM T*t*H-NOX Y140H and 1 mM H_2O_2 at pH 7.5

The second kinetic experiment setup were performed with different H_2O_2 concentrations (0-1 mM) in the presence of 5 mM guaiacol and 3 µM mutant protein.In the control experiment (0 mM H_2O_2) catalytic activity was not observed so it was concluded that the mutant T*t*H-NOX protein only catalayzes the oxidation of guaiacol in the presence of H_2O_2 . As seen in Figure 3.17.b the highest rate observed at 1 mM H_2O_2 efficiency of Y140H mutant varying with H_2O_2 concentration.

At the final kinetic experiment set, guaiacol oxidation by catalyzed 3µM Y140H mutant in presence of 1 mM H_2O_2 were performed under different pH ranges (Figure 3.18.) The highest reaction rate was observed at pH 5.8 (Figure 3.18.b). As in the WT enzyme, the highest activity was observed at pH 5.8. In addition, it was determined that the activity of the mutant enzyme in basic pHs as less than WT.

All kinetic experiment sets for the T*t*H-NOX Y140H were performed in duplicates and the analyses showed that efficiency of mutant Y140H enzyme depends on pH and H_2O_2 concentration and guaiacol concentration.

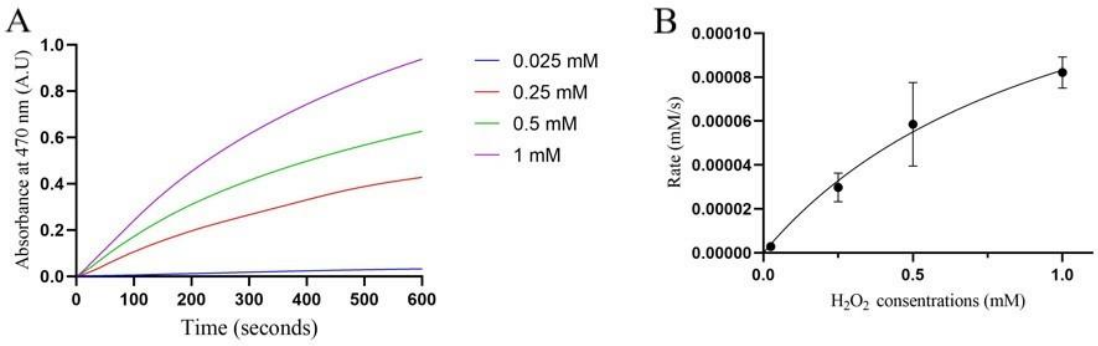

Figure 3.17. (A) Kinetic reactions of T*t*H-NOX Y140H at 470 nm with different H_2O_2 concentrations. (B) Rates of reactions were performed at 25°C between 3 µM T*t*H-NOX Y140H and 5 mM Guaiacol at pH 7.5.

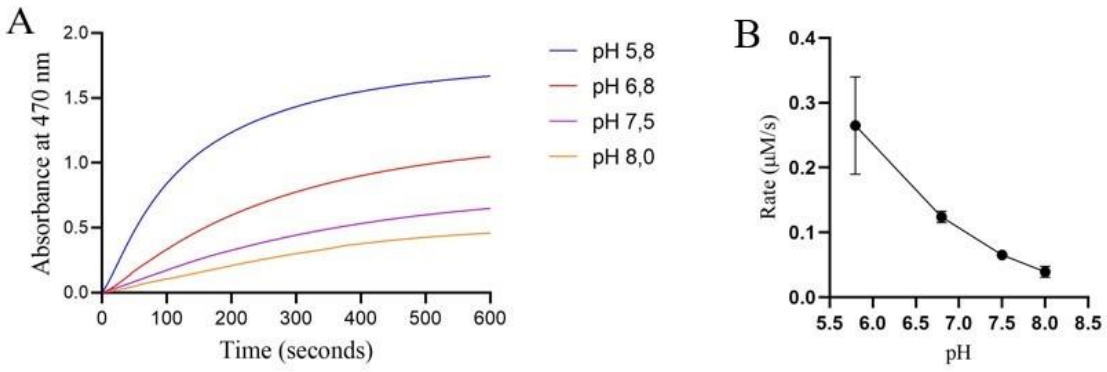

Figure 3.18.(A) Kinetic reactions of T*t*H-NOX Y140H at 470 nm at different pH ranges. (B) Rates of reactions were performed at 25°C between 3 µM T*t*H-NOX Y140H and 5 mM guaiacol in presence of 1 mM H_2O_2 .

3.8.1.5. Kinetic Parameters for the Guaiacol Oxidation

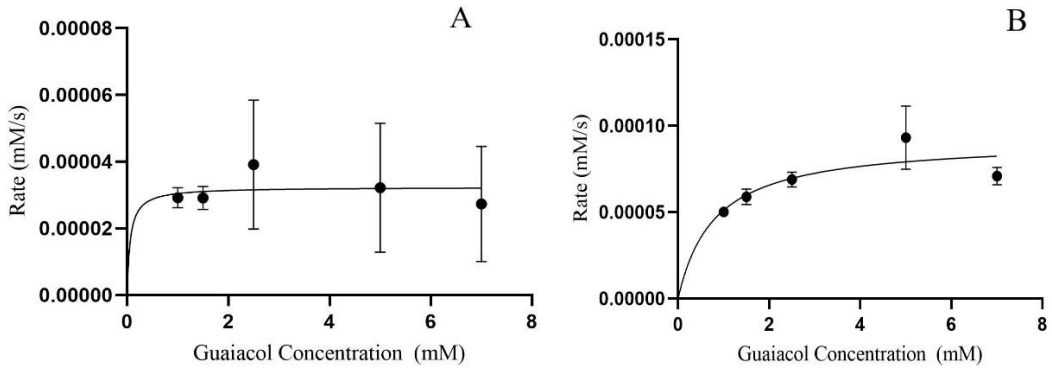

k_{cat}	$1 \pm 0.1 \times 10^{-2}\ s^{-1}$
K_M	0.06 ± 0.3 mM

k_{cat}	$3 \pm 0.3 \times 10^{-2}\ s^{-1}$
K_M	0.7 ± 0.3 mM

Figure 3.19. Kinetic parameters for guaiacol oxidation using (A) WT and (B) Y140H T*t*H-NOX

In order to identify kinetic parameters for guaiacol oxidation, the initial rates was determined at different guaiacol concentrations; (1-7 Mm) with 3 µM WT and Y140H T*t*H-NOX in the presence of 1mM H_2O_2. The turnover number (k_{cat}) for WT and Y140H T*t*H-NOX were determined as $1 \pm 0.1 \times 10^{-2}\ s^{-1}$ and $3 \pm 0.3 \times 10^{-2}\ s^{-1}$ while the K_M was determined to be 0.06 ± 0.3 mM and 0.7 ± 0.3 mM. These results demonstrated that Tetraguaiacol formation was 3-fold faster in the precense of Y140H mutant.

In addition to this, in the presence of increasing concentration of H_2O_2 (0.025-1mM), k_{cat} and K_M was obtanined with 3 µM WT and Y140H T*t*H-NOX and 5 mM guaiacol (Figure 3.20). For the WT k_{cat} was determined as $1 \pm 0.8 \times 10^{-2}\ s^{-1}$ and K_M was determined to be 1.9 ± 1.1 mM. For the Y140H mutant k_{cat} and K_M values was calculated as $5 \pm 2 \times 10^{-2}\ s^{-1}$ and 1.9 ± 1.1 mM.

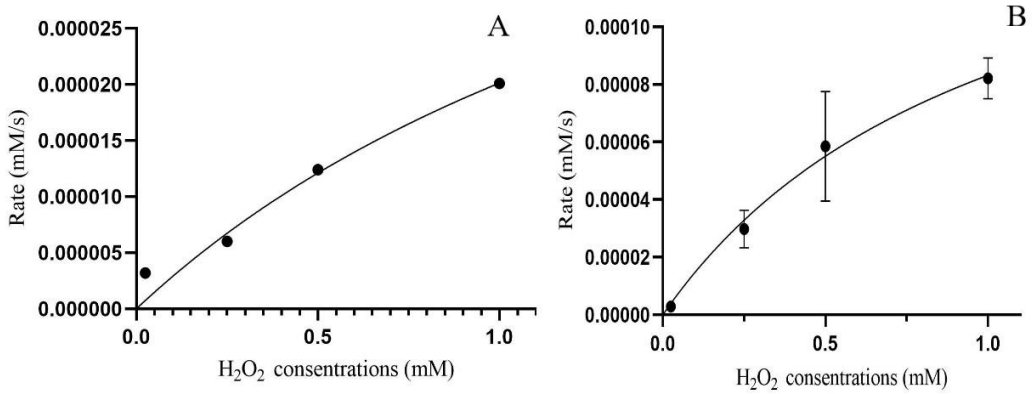

K_M	1.9 ± 1.1 mM
k_{cat}	1 ± 0.8 x 10^{-2} s^{-1}

K_M	1.9 ± 1.1 mM
k_{cat}	5 ± 2x10^{-2} s^{-1}

Figure 3.20. Kinetic parameters of guaiacol oxidation in the presence of increasing concentration of H_2O_2 (0.025 -1mM). (A) With WT. (B) With Y140H mutant.

3.8.2. Catalyic activity of T*t*H-NOX protein towards Amplex Red Oxidation

In literature, amplex red and HRP combination mostly use for the detection of H_2O_2 that released from biological samples including cells or generated in enzyme-coupled reactions. In the presence of H_2O_2, amplex red can be oxidized by the T*t*H-NOXs and the red-fluorescent oxidation product resorufin is produced as seenin the Equation 2.

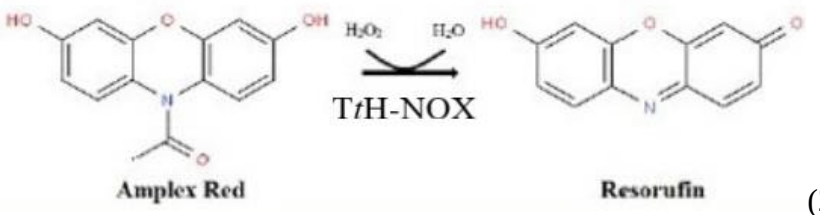

(2)

Oxidation of 10 µM Amplex Red by TtH-NOX proteins were performed with 1.5 µM protein in the presence of 1.5 µM H_2O_2 at 50 Mm Kpi pH 7.5. Formation of resorufin was followed at 570 nm during the reaction WT (A) and Y140H mutant (B) were oxidized

amplex red in the presence of H_2O_2. As seen in Figure 3.21.b WT T*t*H-NOX was catalyzed the reaction very rapidly and in six minutes formation absorbance was reached maximum. After this time point absorbance at 570 nm was decreased gradually. As seen in Figure 3.20.d, the amplex red oxidation catalyzed by Y140H mutant protein was reached the maximum formation absorbance in two minutes. While the absorbance at 570 nm increased during the reaction, the soret peak at 410 nm decreased and flattened (Figure 3.21.b).

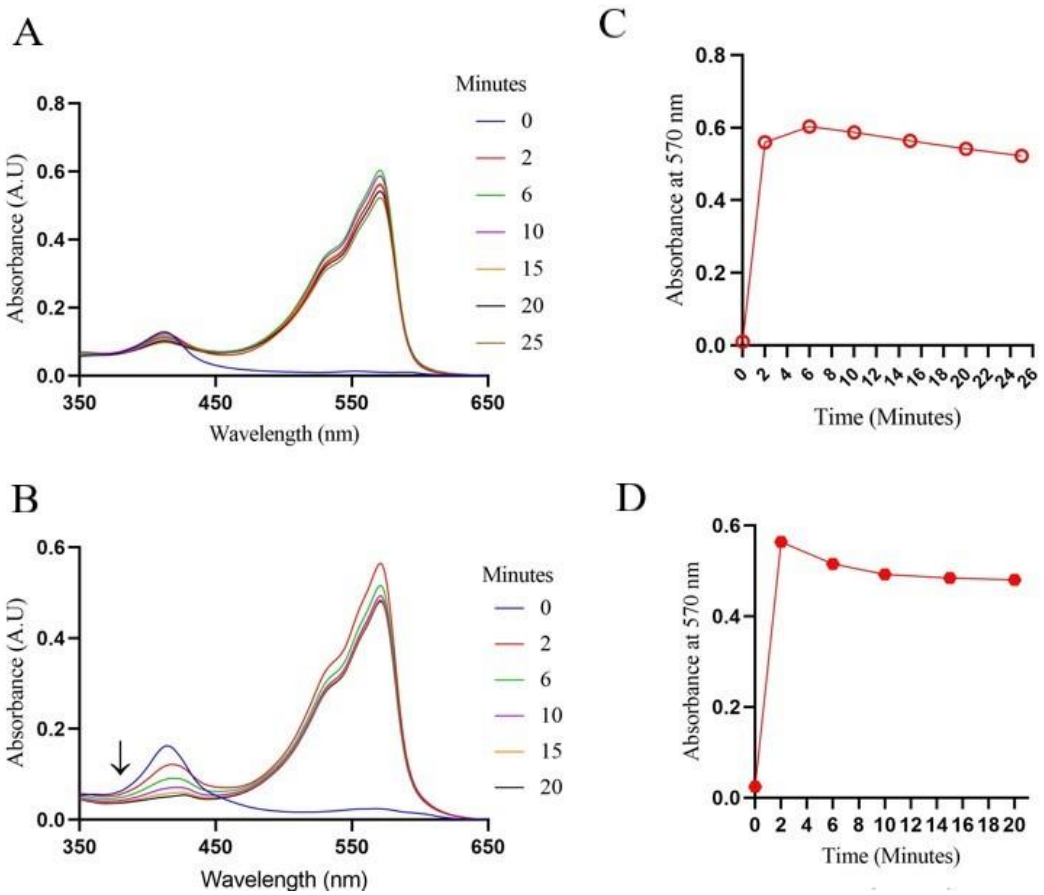

Figure 3.21. (A) WT and (B) Y140H TtH-NOX were catalyzed Amplex Red oxidations in the presence of H_2O_2. Resorufin formation at 570 nm with time catalyzed by WT(C) and Y140H mutant (D).

These results showed that although there are slight differences, the amplex red oxidation catalyzed by T*t*H-NOX proteins is similar to the oxidation reaction performed with N-His CYP119. In the reaction catalyzed by N-His CYP119, the absorbance at 570

nm increases while the soret at 415 nm decreases during the reaction (Aslantas and Surmeli, 2019).

3.8.3. Kinetic Parameters for the Amplex Red Oxidation

In the presence of increasing concentrations of H_2O_2 (0.25 -2 mM),turnover number (k_{cat}) and K_M was determined for the amplex red oxidations that catalyzed by 1.5 µM T*t*H-NOX enzyme with the 10 µM Amplex red at pH 7.5. Turnover number (k_{cat}) for WT and Y140H T*t*H-NOX were determined as 0.14 ± 0.07 s^{-1} and 0.1 ± 0.01 s^{-1} while the K_M was determined to be 2.02 ± 1.8 mM and 0.6 ± 0.2 mM, respectively.

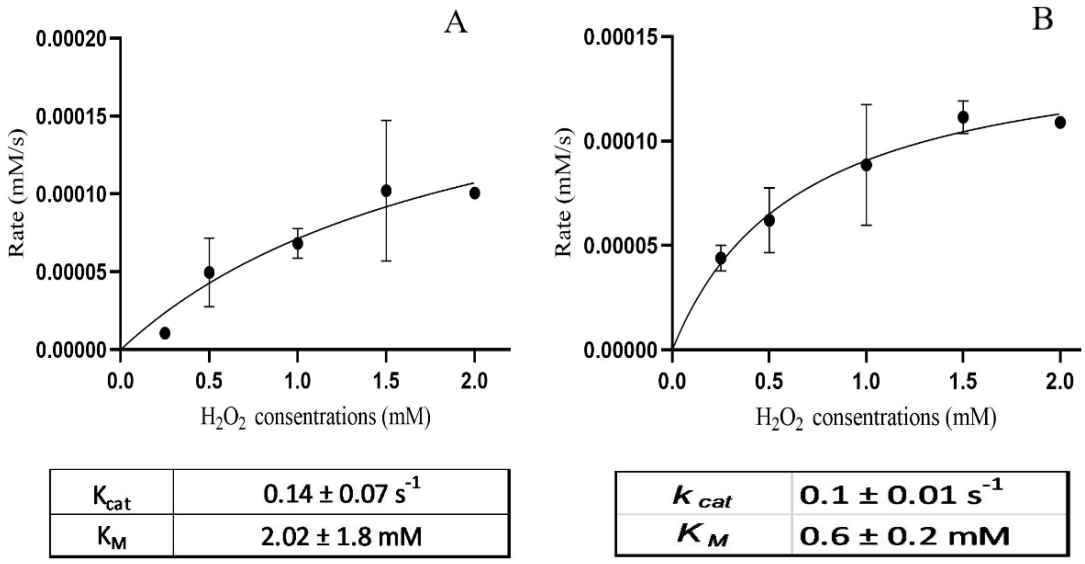

Figure 3.22. Kinetic parameters for Amplex Red oxidation at different H_2O_2 (0.25 -2 mM) concentrations. (A) With WT. (B) With Y140H mutant.

3.8.4. Catalyic activity of T*t*H-NOX Y140H towards ABTS oxidation

The one-electron oxidation of 2,2'-azino-bis(3-ethylbenzthiazoline-6-sulfonic acid) (ABTS) into the green radical cation, $ABTS^{\bullet+}$ was performed with 0.5 µM mutant T*t*H-NOX enzyme in the presence of 1 mM ABTS and 1mM H_2O_2 at pH 7.5 (50 mM potassium phosphate). The formation of $ABTS^{\bullet+}$ was occurred as seen in equation 3 and were followed at 736 nm at room temperature.

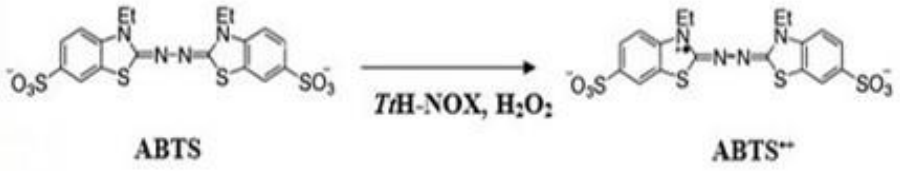

(3)

As illustrated in Figure 3.22 in the presence of H_2O_2 Y140H mutant was catalyzed the ABTS oxidation and the reaction was completed in 10 minutes.

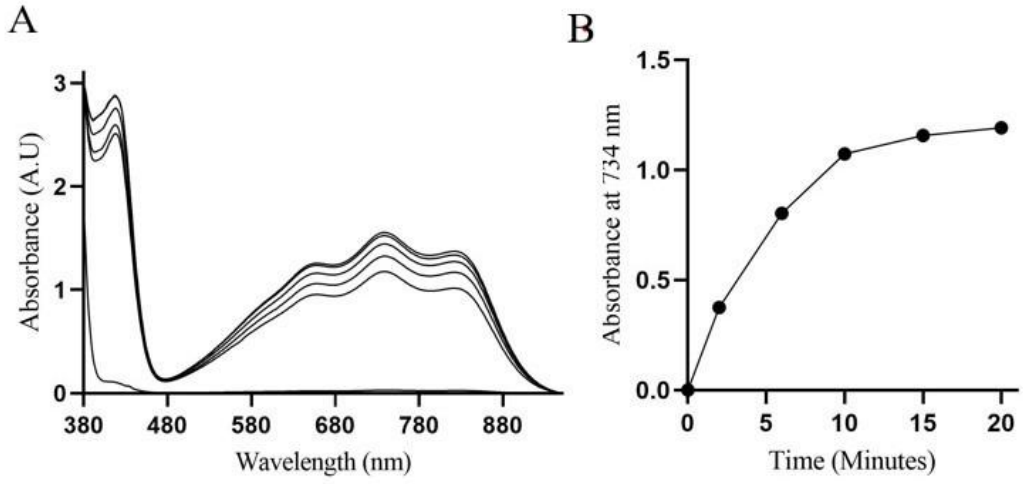

Figure 3.23 ABTS oxidation reaction catalyzed by Y140H mutant (A). Formation of $ABTS^{\bullet+}$ at 734 nm with time (B).

3.8.5. Kinetic Parameters for the ABTS Oxidation

In order to determine kinetic parameters for 2,2'-azino-bis(3-ethylbenzthiazoline-6-sulfonicacid)(ABTS) oxidation which catalyzed by Y140H T*t*H-NOX, kinetic reactions were performed with 1µM enzyme with different ABTS concentrations (0.1- 1mM) in the presence of 1mM H_2O_2 at pH 7.5 (50 Mm potassium phosphate).

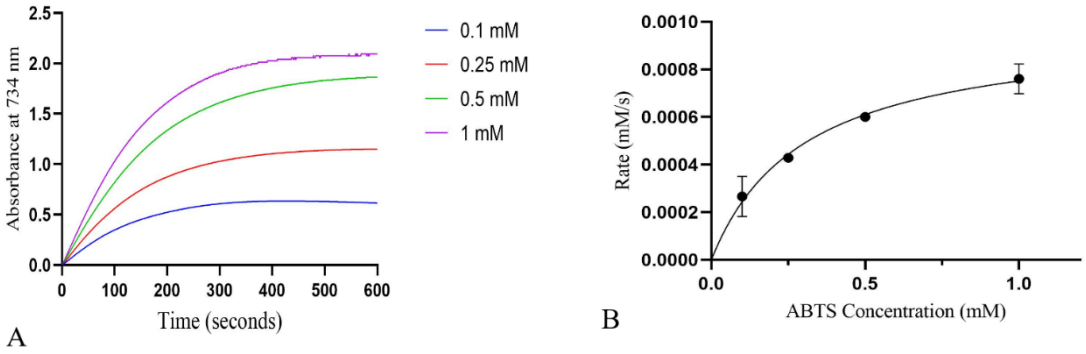

K_M	0.3 ± 0.06 mM
k_{cat}	0.9 ± 0.07 s^{-1}

C

Figure 3.24. Kinetic experiments for the ABTS oxidation catalyzed by Y140H T*t*H-NOX. (A) Reaction profiles of Y140H T*t*H-NOX at 734 nm with different ABTS concentrations. (B) Rates of reactions at different ABTS concentrations. (C) K_M and k_{cat} values .

The turnover number (k_{cat}) for Y140H T*t*H-NOX was determined as 0.9 ± 0.07 s^{-1} and K_M was determined as 0.3 ± 0.06 mM. In the previous study of Aggrey-Fynn and Surmeli, 2018, K_M for WT T*t*H-NOX was determined as 0.74 ± 0.13 mM and k_{cat} determined to be 0.06 ± 0.02 s^{-1}.

Compared results showed that Y140H mutant catalysed the reaction 15 - fold faster than WT and also showed higher affinity for ABTS.

3.9. T*t*H-NOX proteins Stability in the presence of Organic solvent

Stability of T*t*H-NOX protein were investigated with the amplex red peroxidase reactions that were performed in the presence of 2.5 % and 5 % organic solvent. Results demonstrated that stability of WT T*t*H-NOX has not changed significantly with increasing amount of organic solvent. Also, the stability of WT protein in the methanol, ethanol and acetonitrile gave similar results (Figure 3.25)

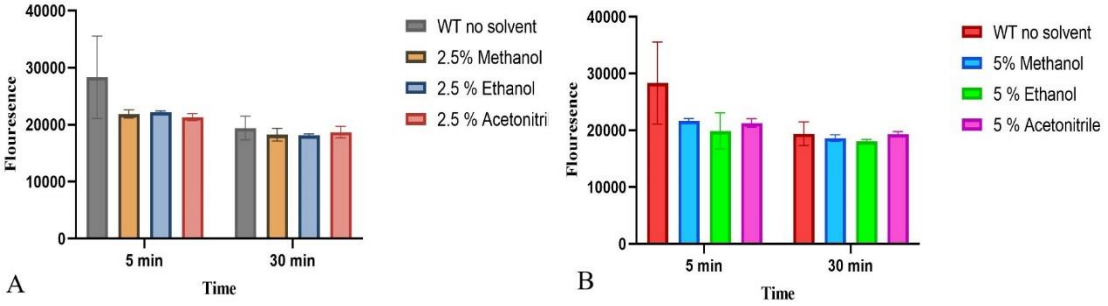

Figure 3.25. Stability of WT T*t*H-NOX at different organic solvent. Stability in the presence of 2.5% (A) and 5 % (B)

Y140H T*t*H-NOX's stability was showed similar results to WT TtH-NOX. Stability of the mutant protein was not significantly different at 2.5 % and 5 % organic solvent. In addition to this at different organic solvent stability showed similar results.(Figure 3.26.)

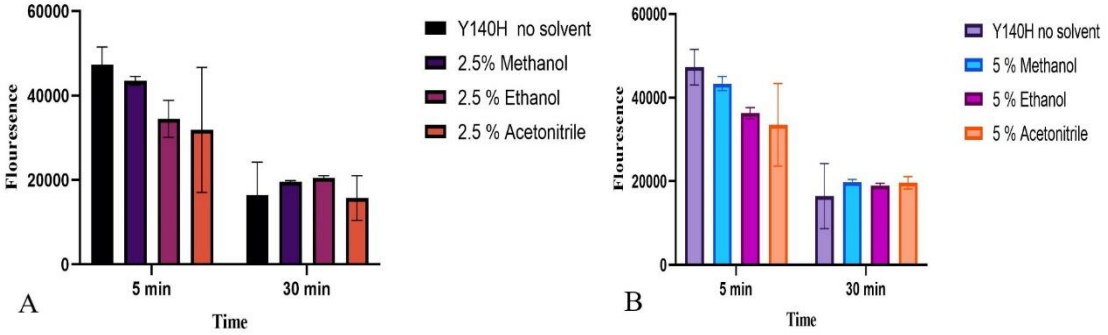

Figure 3.26. Stability of Y14OH T*t*H-NOX at different organic solvent. Stability in the presence of 2.5% (A) and 5 % (B)

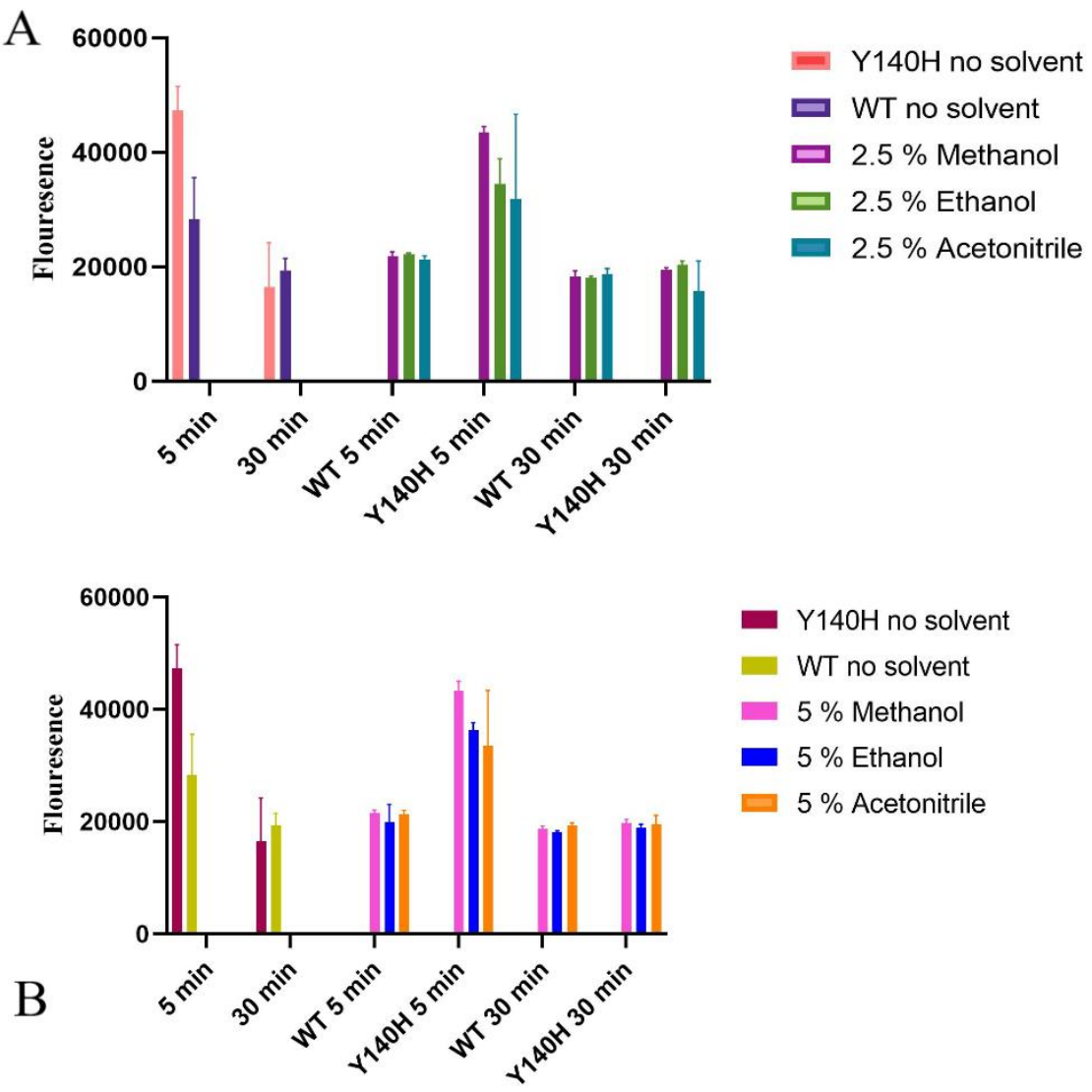

Figure 3.27. Stability comparison of WT and Y140H T*t*H-NOX in the presence of organic solvent. (A) 2.5 % and (B) 5 %

As seen in the Figure 3.26, in the presence of both 2.5 % and 5 % organic solvent, WT protein was more stable than Y140H mutant.

CHAPTER 4

CONCLUSION

Enzymes are magnificent biomolecules that can perform many different functions that are vital to all life forms in nature. These structures, which have provided us with a lot of practicality in daily life and industrial areas since ancient times, can be further developed and strengthened thanks to the opportunities offered by biotechnology and the important developments in protein engineering. Enzyme engineering not only provides durability, desired purity, high efficiency and comfortable operation under any desired conditions, but it also makes possible to create an environmentally friendly and sustainable system. Hemoproteins take part in different biological processes in many stages of life. Their ability to catalyze important biosynthesis reactions makes them good candidates for understanding and elucidating complex mechanisms for biocatalysis.

In this study, the catalytic properties of thermophilic T*t*H-NOX protein, a heme protein was reshaped by rational design. The designed Y140H mutant; was investigated and chemical characterization of mutant and wild type enzyme was carried out. The peroxidase activity of the enzyme was investigated by the oxidation reactions of guaiacol, amplex red and ABTS which were not used as substrate before. At the same time, guaiacol and amplex red reactions were also carried with the wild type enzyme to understand the effects of mutations.

In the presence of hydrogen peroxide both WT and Y140H T*t*H-NOX catalyzed guaiacol oxidation efficiently. In order to make more accurate observations in terms of kinetics, three different kinetic experiment sets have been carried out in different environmental conditions. This allowedus to the effects of substrate,concentration and pH on reaction kinetics.

For wild type enzyme, it was observed that enzyme efficiency was affected by changes in pH and different guaiacol and hydrogen peroxide concentrations. While no reaction is observed in the absence of hydrogen peroxide with the increasing concentration of hydrogen peroxide, the reaction accelerated. There was no significant

difference between the reaction rates in the pH values tested, while it was observed that the reaction rate was maximum at pH 5.8.

When the same conditions were examined in the Y140H mutant, it was seen that the reaction was affected by changing pH and concentrations. The reaction rate increased with increasing guaiacol and hydrogen peroxide concentrations and the highest concentration was observed at the highest concentration of hydrogen peroxide. The highest rate was observed at pH 5.8 for the mutant enzyme as like wild type.

Differences were observed in the spectra of both enzymes taken during the guaiacol oxidation. In the oxidation reaction catalyzed by the WT enzyme, the absorbance at 415 nm was increased and a wide band formation was observed at 470 nm. The reaction was completed in 20 minutes. On the other hand, the absorbance of the mutant enzyme at 410 nm increased during the first 20 minutes and then decreased and began to lose its sharpness, and the reaction was completed in 10 minutes.

Kinetic parameters of the guaiacol oxidation was investigated for both WT and Y140H mutant. The turnover number (k_{cat}) for WT and Y140H T*t*H-NOX were determined as $1 \pm 0.1 \times 10^{-2}$ s^{-1} and $3 \pm 0.3 \times 10^{-2}$ s^{-1} while the K_M was determined to be 0.06 ± 0.3 mM and 0.7 ± 0.3 mM, respectively. It is concluded that tetraguaiacol formation was 3-fold faster in the presence of Y140H mutant. In addition, in the presence of increasing concentrations of H_2O_2, k_{cat} was determined $1 \pm 0.8 \times 10^{-2}$ s^{-1} and K_M was determined to be 1.9 ± 1.1 mM. For the Y140H mutant k_{cat} and K_M values was calculated as $5 \pm 2 \times 10^{-2}$ s^{-1} and 1.9 ± 1.1 mM.

For the first time, oxidation of amplex red catalyzed by T*t*H-NOXs were investigated. WT and Y140H mutant oxidized amplex red in the presence of H_2O_2 efficiently. WT T*t*H-NOX catalyzed the reaction in six minutes and Y140H mutant catalyzed in two minutes.The kinetic parameters k_{cat} and K_M values were determined in the presence of increasing concentrations of H_2O_2. The turnover number k_{cat} for WT and Y140H T*t*H-NOX were determined as 0.14 ± 0.07 s^{-1} and 0.1 ± 0.01 s^{-1} while K_M was determined as 2.02 ± 1.8 mM and 0.6 ± 0.2 mM, respectively.

Oxidation of ABTS with Y140H mutant was also performed. In the presence of hydrogen peroxide mutant enzyme catalyzed the reaction and was completed in 10 minutes. Kinetic parameters were determined as k_{cat} 0.9 ± 0.07 s^{-1} and K_M 0.3 ± 0.06 mM for ABTS. When the results compared with WT, Y140H mutant catalyzed the reaction 15 - fold faster than WT and also showed higher affinity for ABTS.

Stability of T*t*H-NOX proteins in the precense of organic solvent was investigated. In the presence of 2.5 % and - 5 % organic solvent the stability of WT and Y140H T*t*H-NOX were not changed significantly. Three organic solvents were used for stability tests methanol, ethanol and acetonitrile the stability did not change significantly for the solvents tested. Results demonstrated that WT T*t*H-NOX was more stable than Y140H mutant in the presence of organic solvents.

For the first time, copper ion incorporated T*t*H-NOX-based hybrid nanoflowers were synthesized in this study. SEM and EDX analysis of T*t*H-NOX-based hybrid nanoflowers proved that free T*t*H-NOXs were immobilized successfully.

In conclusion, this study has shown that T*t*H-NOX proteins are capable of the oxidizing guaiacol, amplex red and ABTS. Y140H T*t*H-NOX catalyzed oxidation of guaiacol and ABTS more efficiently than WT. Also, for the first-time formation of T*t*H-NOX-based hybrid nanoflowers was shown. However, to further investigate nanoflowers catalytic potentials, oxidation reactions with guaiacol, amplex red and ABTS should be performed.

REFERENCES

Abedi, D. 2011. “Enzyme Biocatalysis.” In *Comprehensive Biotechnology*. Amsterdam ; Boston: Elsevier.

Aggrey-Fynn, Joana Efua, and Nur Basak Surmeli. 2018. “A Novel Thermophilic Hemoprotein Scaffold for Rational Design of Biocatalysts.” *JBIC Journal of Biological Inorganic Chemistry* 23 (8): 1295–1307.

Albrecht Messerschmidt. 2001. *Handbook of Metalloproteins. Vol. 2*. Chichester Wiley.

Altınkaynak, Cevahir, and Nalan Özdemir. 2016. “A New Generation Approach in Enzyme Immobilization: Organic-Inorganic Hybrid Nanoflowers with Enhanced Catalytic Activity and Stability.” *Enzyme and Microbial Technology,*

Animesh Goswami, and Jon D Stewart. 2016. *Organic Synthesis Using Biocatalysis*. Amsterdam: Elsevier.

Aono, Shigetoshi, Toshiyuki Kato, Mayumi Matsuki, Hiroshi Nakajima, Takehiro Ohta, Takeshi Uchida, and Teizo Kitagawa. 2002. “Resonance Raman and Ligand Binding Studies of the Oxygen-Sensing Signal Transducer Protein HemAT FromBacillus Subtilis.” *Journal of Biological Chemistry* 277 (16): 13528–38.

Asano, Yasuhisa, Takamune Yasuda, Yoshiki Tani, and Hideaki Yamada. 1982. “A New Enzymatic Method of Acrylamide Production.” *Agricultural and Biological Chemistry* 46 (5): 1183–89.

Aslantas, Yaprak, and Nur Basak Surmeli. 2019. “Effects of N-Terminal and C-Terminal Polyhistidine Tag on the Stability and Function of the Thermophilic P450 CYP119.” *Bioinorganic Chemistry and Applications* 2019 (June): 1–8.

Bilal, Muhammad, and Muhammad Asgher. 2019. “Engineering Enzyme-Coupled Hybrid Nanoflowers: The Quest for Optimum Performance to Meet Biocatalytic Challenges and Opportunities.” *International Journal of Biological Macromolecules*.

Boon, Elizabeth M, and Michael A Marletta. 2005. “Ligand Discrimination in Soluble Guanylate Cyclase and the H-NOX Family of Heme Sensor Proteins.” *Current Opinion in Chemical Biology* 9 (5): 441–46.

Booth, WilliamT., Caleb R. Schlachter, Swanandi Pote, Nikita Ussin, Nicholas J. Mank, Vincent Klapper, Lesa R. Offermann, Chuanbing Tang, Barry K. Hurlburt, and Maksymilian Chruszcz. 2018. “Impact of an N-Terminal Polyhistidine Tag on Protein Thermal Stability.” *ACS Omega* 3 (1): 760–68.

Bornhorst, J A, and J J Falke. 2000. “Purification of Proteins Using Polyhistidine Affinity Tags.” *Methods in Enzymology* 326: 245–54.

Bornscheuer, U T, and R J Kazlauskas. 2006. *Hydrolases in Organic Synthesis : Regio- and Stereoselective Biotransformations*. Weinheim: Wiley-Vch ; Chichester.

Bowman, Sarah E. J., and Kara L. Bren. 2008. “The Chemistry and Biochemistry of Heme C: Functional Bases for Covalent Attachment.” *Natural Product Reports* 25 (6): 1118–30.

Carlson, H. K, and R. E Vance,. 2010. “H-NOX Regulation of C-Di-GMP Metabolism and Biofilm Formation in Legionella Pneumophila. 77(4), 930–942.” *Molecular Microbiology*.

Chance, Britton, and A.C. Maehly. 1955. “[136] Assay of Catalases and Peroxidases.” *Methods in Enzymology* 2 (): 764–75.

Cui, Jiandong, and Shiru Jia. 2017. “Organic–Inorganic Hybrid Nanoflowers: A Novel Host Platform for Immobilizing Biomolecules.” *Coordination Chemistry Reviews* 352 (December): 249–63.

Dai, Zhou, and Elizabeth M. Boon. 2010. “Engineering of the Heme Pocket of an H-NOX Domain for Direct Cyanide Detection and Quantification.” *Journal of the American Chemical Society* 132 (33): 11496–503.

Datta, Sumitra, L. Rene Christena, and Yamuna Rani Sriramulu Rajaram. 2012. “Enzyme Immobilization: An Overview on Techniques and Support Materials.” *3 Biotech* 3 (1): 1–9.

Denninger, John W, and Michael A Marletta. 1999. “Guanylate Cyclase and the ·NO/CGMP Signaling Pathway.” *Biochimica et Biophysica Acta (BBA) - Bioenergetics* 1411 (2-3): 334–50.

Diaz, Juan E., Chun-Shi Lin, Kazuyoshi Kunishiro, Birte K. Feld, Sara K. Avrantinis, Jonathan Bronson, John Greaves, Jeffery G. Saven, and Gregory A. Weiss. 2011. “Computational Design and Selections for an Engineered, Thermostable Terpene Synthase.” *Protein Science* 20 (9): 1597–1606.

Diederix, Rutger E. M., Marcellus Ubbink, and Gerard W. Canters. 2001. “The Peroxidase Activity of Cytochrome c-550 from Paracoccus Versutus.” *European Journal of Biochemistry* 268 (15): 4207–16.

Dinçer, Ayşe, and Azmi Telefoncu. 2007. “Improving the Stability of Cellulase by Immobilization on Modified Polyvinyl Alcohol Coated Chitosan Beads.” *Journal of Molecular Catalysis B: Enzymatic* 45 (1-2): 10–14.

Escobar, Sindy, Susana Velasco-Lozano, Chih-Hao Lu, Yu-Feng Lin, Monica Mesa, Claudia Bernal, and Fernando López-Gallego. 2017. “Understanding the Functional Properties of Bio-Inorganic Nanoflowers as Biocatalysts by Deciphering the Metal-Binding Sites of Enzymes.” *Journal of Materials Chemistry B* 5 (23): 4478–86.

Everse, J. 2013. “Heme Proteins.” *Encyclopedia of Biological Chemistry*, 532–38.

Ge, Jun, Jiandu Lei, and Richard N. Zare. 2012. “Protein–Inorganic Hybrid Nanoflowers.” *Nature Nanotechnology* 7 (7): 428–32.

Gilles-Gonzalez, Marie A., Gary S. Ditta, and Donald R. Helinski. 1991. “A Haemoprotein with Kinase Activity Encoded by the Oxygen Sensor of Rhizobium Meliloti.” *Nature* 350 (6314): 170–72.

Granick, S., and A. Kappas. 1967. “Steroid Control of Porphyrin and Heme Biosynthesis: A New Biological Function of Steroid Hormone Metabolites.” *Proceedings of the National Academy of Sciences* 57 (5): 1463–67.

Graslund,. 2008. “Protein Production and Purification.” *Nature Methods* 5 (2): 135–46.

Guengerich, F. Peter. 2007. “Mechanisms of Cytochrome P450 Substrate Oxidation: MiniReview.” *Journal of Biochemical and Molecular Toxicology* 21 (4): 163–68.

Hare, Joshua M., and Wilson S. Colucci. 1995. “Role of Nitric Oxide in the Regulation of Myocardial Function.” *Progress in Cardiovascular Diseases* 38 (2): 155–66.

Hartmeier, Winfried. 2012. *Immobilized Biocatalysts: An Introduction*. *Google Books*. Springer Science & Business Media.

He, Xiaohui. 2017. “Self-Assembled Metalloporphyrins–Inorganic Hybrid Flowers and Their Application to Efficient Epoxidation of Olefins.” *Chemical Technology and Biotechnology* 92 (10).

Homaei, Ahmad Abolpour, Reyhaneh Sariri, Fabio Vianello, and Roberto Stevanato. 2013. “Enzyme Immobilization: An Update.” *Journal of Chemical Biology* 6 (4): 185–205.

Hossain, Sajjad, Ilana Heckler, and Elizabeth M. Boon. 2018. “Discovery of a Nitric Oxide Responsive Quorum Sensing Circuit in Vibrio Cholerae.” *ACS Chemical Biology* 13 (8): 1964–69.

IUPAC. 1997. “IUPAC Compendium of Chemical Terminology.” Edited by Miloslav Nič, Jiří Jirát, Bedřich Košata, Aubrey Jenkins, and Alan McNaught, June.

Iyer, LM, V Anantharaman, and L Aravind. 2003. “Ancient Conserved Domains Shared by Animal Soluble Guanylyl Cyclases and Bacterial Signaling Proteins.” *BMC Genomics.* 3.

Jain, Rinku, and Michael K. Chan. 2003. “Mechanisms of Ligand Discrimination by Heme Proteins.” *JBIC Journal of Biological Inorganic Chemistry* 8 (1): 1–11.

Jia, Feng, Balaji Narasimhan, and Surya Mallapragada. 2013. “Materials-Based Strategies for Multi-Enzyme Immobilization and Co-Localization: A Review.” *Biotechnology and Bioengineering* 111 (2): 209–22.

Jin, Kyoungsuk. 2014. “Hydrated Manganese(II) Phosphate ($Mn_3(PO_4)_2 \cdot 3H_2O$) as a Water Oxidation Catalyst.” *J Am Chem Soc . 2014 May*.

Karlheinz Drauz. 2012. *Enzyme Catalysis in Organic Synthesis 1*. Weinheim Wiley-Vch.

Ke, C., Y. Fan, Y. Chen, L. Xu, and Y. Yan. 2016. “A New Lipase–Inorganic Hybrid Nanoflower with Enhanced Enzyme Activity.” *RSC Advances* 6 (23): 19413–16.

Khan, Kishore Kuman, Madhu Sudan Mondal, Lakshmichand Padhy, and Samaresh Mitra. 1998. “The Role of Distal Histidine in Peroxidase Activity of Myoglobin. Transient-Kinetics Study of the Reaction of H_2O_2 with Wild-Type and Distal-Histidine-Mutanted Recombinant Human Myoglobin.” *European Journal of Biochemistry* 257 (3): 547–55.

Kragl, Udo, Lasse Greiner, and Christian Wandrey. 2002. “Enzymes, Immobilized, Reactors.” *Encyclopedia of Bioprocess Technology*, October.

Kumar, Ashok, In-Won Kim, Sanjay K. S. Patel, and Jung-Kul Lee. 2017. “Synthesis of Protein-Inorganic Nanohybrids with Improved Catalytic Properties Using Co3(PO4)2.” *Indian Journal of Microbiology* 58 (1): 100–104.

Lee, Hye Rin, Minsoo Chung, Moon Il Kim, and Sung Ho Ha. 2017. “Preparation of Glutaraldehyde-Treated Lipase-Inorganic Hybrid Nanoflowers and Their Catalytic Performance as Immobilized Enzymes.” *Enzyme and Microbial Technology* 105 (October): 24–29.

Lemière, G.L., J.A. Lepoivre, and F.C. Alderweireldt. 1985. “Hlad-Catalyzed Oxidations of Alcohols with Acetaldehyde as a Coenzyme Recycling Substrate.” *Tetrahedron Letters* 26 (37): 4527–28.

Liese, A, K Seelbach, and Christian Wandrey. 2006. *Industrial Biotransformations*. Weinheim: Wiley-Vch.

Luetz, Stephan, Lori Giver, and James Lalonde. 2008. “Engineered Enzymes for Chemical Production.” *Biotechnology and Bioengineering* 101 (4): 647–53.

Majorek, Karolina A., Misty L. Kuhn, Maksymilian Chruszcz, Wayne F. Anderson, and Wladek Minor. 2014. “Double Trouble-Buffer Selection and His-Tag Presence May Be Responsible for Nonreproducibility of Biomedical Experiments.” *Protein Science* 23 (10): 1359–68.

Meryam Sardar, Razi Ahmad. 2015. “Enzyme Immobilization: An Overview on Nanoparticles as Immobilization Matrix.” *Biochemistry & Analytical Biochemistry* 04 (02).

Mohamad, Nur Royhaila, Nur Haziqah Che Marzuki, Nor Aziah Buang, Fahrul Huyop, and Roswanira Abdul Wahab. 2015. “An Overview of Technologies for Immobilization of Enzymes and Surface Analysis Techniques for Immobilized Enzymes.” *Biotechnology & Biotechnological Equipment* 29 (2): 205–20.

Ocsoy, Ismail. 2015. “A New Generation of Flowerlike Horseradish Peroxides as a Nanobiocatalyst for Superior Enzymatic Activity.” *Enzyme and Microbial Technology* Volumes 75–76,.

Ow, Yong-Ling P., Douglas R. Green, Zhenyue Hao, and Tak W. Mak. 2008. “Cytochrome C: Functions beyond Respiration.” *Nature Reviews Molecular Cell Biology* 9 (7): 532–42.

Panek, Anna, Olga Pietrow, Paweł Filipkowski, and Józef Synowiecki. 2013. “Effects of the Polyhistidine Tag on Kinetics and Other Properties of Trehalose Synthase from Deinococcus Geothermalis.” *Acta Biochimica Polonica* 60 (2).

Pellicena, Patricia, and S. Karow. 2004. “Crystal Structure of an Oxygen-Binding Heme Domain Related to Soluble Guanylate Cyclases.” *PNAS*.

Plate, Lars, and Michael A. Marletta. 2013. “Nitric Oxide-Sensing H-NOX Proteins Govern Bacterial Communal Behavior.” *Trends in Biochemical Sciences* 38 (11): 566–75.

Poulos, Thomas L. 2014. “Heme Enzyme Structure and Function.” *Chemical Reviews* 114 (7): 3919–62.

Rasheed, Tahir, Chuanlong Li, Muhammad Bilal, Chunyang Yu, and Hafiz M.N. Iqbal. 2018. “Potentially Toxic Elements and Environmentally-Related Pollutants Recognition Using Colorimetric and Ratiometric Fluorescent Probes.” *Science of the Total Environment* 640-641 (November): 174–93.

Reedy, Charles J., and Brian R. Gibney. 2004. “Heme Protein Assemblies.” *ChemInform* 35 (20).

Reichlin, M. 1972. “Hemoglobin and Myoglobin in Their Reactions with Ligands. Eraldo Antonini and Maurizio Brunori. North-Holland, Amsterdam, 1971 (U.S. Distributor, Elsevier, New York). Xx, 436 Pp., Illus. $30. Frontiers of Biology, Vol. 21.” *Science* 178 (4058): 296–96.

Rozzell, J.David. 1999. “Commercial Scale Biocatalysis: Myths and Realities.” *Bioorganic & Medicinal Chemistry* 7 (10): 2253–61.

Sabaty, Monique, Sandrine Grosse, Geraldine Adryanczyk, Séverine Boiry, Frédéric Biaso, Pascal Arnoux, and David Pignol. 2013. “Detrimental Effect of the 6 His C-Terminal Tag on YedY Enzymatic Activity and Influence of the TAT Signal Sequence on YedY Synthesis.” *BMC Biochemistry* 14 (1): 28.

Servi, Stefano. 1990. “Baker’s Yeast as a Reagent in Organic Synthesis.” *Synthesis* 1990 (01): 1–25.

Shelver, D., R. L. Kerby, Y. He, and G. P. Roberts. 1997. “CooA, a CO-Sensing Transcription Factor from Rhodospirillum Rubrum, Is a CO-Binding Heme Protein.” *Proceedings of the National Academy of Sciences* 94 (21): 11216–20.

Shichi, Hitoshi. 1969. “Microsomal Electron Transfer System of Bovine Retinal Pigment Epithelium.” *Experimental Eye Research* 8 (1): 60–68.

Somturk, Burcu, and Nalan Özdemir. 2015. “Synthesis of Copper Ion Incorporated Horseradish Peroxidase-Based Hybrid Nanoflowers for Enhanced Catalytic Activity and Stability.” *Dalton Trans.* , 2015,44, 13845-13852.

Sun, Jiayu, Jiechao Ge, Weimin Liu, Minhua Lan, Hongyan Zhang, Pengfei Wang, Yanming Wang, and Zhongwei Niu. 2014. “Multi-Enzyme Co-Embedded Organic–Inorganic Hybrid Nanoflowers: Synthesis and Application as a Colorimetric Sensor.” *Nanoscale* 6 (1): 255–62..

Toda, Noboru, and Tomio Okamura. 2003. “The Pharmacology of Nitric Oxide in the Peripheral Nervous System of Blood Vessels.” *Pharmacological Reviews* 55 (2): 271–324.

Tran, Tai Duc, and Moon Il Kim. 2018. “Organic-Inorganic Hybrid Nanoflowers as Potent Materials for Biosensing and Biocatalytic Applications.” *BioChip Journal* 12 (4): 268–79.

Trudeau, Devin L., Toni M. Lee, and Frances H. Arnold. 2014. “Engineered Thermostable Fungal Cellulases Exhibit Efficient Synergistic Cellulose Hydrolysis at Elevated Temperatures.” *Biotechnology and Bioengineering* 111 (12): 2390–97.

Underbakke, E.S, and N.B Surmeli. 2013. “Nitric Oxide Signaling.”

Wandrey, Christian, Andreas Liese, and David Kihumbu. 2000. “Industrial Biocatalysis: Past, Present, and Future.” *Organic Process Research & Development* 4 (4): 286–90.

Wu, Zhuofu, and Xiang Li. 2014. “Enantioselective Transesterification of (R,S)-2-Pentanol Catalyzed by a New Flower-like Nanobioreactor.” *RSC Advances*,.

Xu, Zheng, Rui Wang, Chao Liu, Bo Chi, Jian Gao, Beining Chen, and Hong Xu. 2016. “A New L-Arabinose Isomerase with Copper Ion Tolerance Is Suitable for Creating Protein–Inorganic Hybrid Nanoflowers with Enhanced Enzyme Activity and Stability.” *RSC Advances* 6 (37): 30791–94.

Zhang, Yifei, Jun Ge, and Zheng Liu. 2015. “Enhanced Activity of Immobilized or Chemically Modified Enzymes.” *ACS Catalysis* 5 (8): 4503–13.

APPENDIX

AMINO ACID SEQUENCES

Wild type *Tt*H-NOX:

HMKGTIVGTWIKTLRDLYGNDVVDESLKSVGWEPDRVITPLEDIDDDEV
RRIFAKVSEKTGKNVNEIWREVGRQNIKTFSEWFPSYFAGRRLVNFLMMMDEV
HLQLTKMIKGATPPRLIAKPVAKDAIEMEYVSKRKMYDYFLGLIEGSSKFFKEEI
SVEEVERGEKDGFSRLKVRIKFKNPVFEYKKNLEHHHHHH

Y140H *Tt*H-NOX:

HMKGTIVGNWIKTLRDLYGNDVVDESLKSVGWEPDRVITPLEDIDDDEVRRIFA
KVSEKTGKNVNEIWREVGRQNIKTFSEWFPSYFAGRRLVNFLMMMDEVHLQL
TKMIKGATPPRLIAKPVAKDAIEMEYVSKRKMYDHFLGLIEGSSKFFKEEISVEE
VERGEKDGFSRLKVRIKFKNPVFEYKKNLEHHHHHH